Research Square

Preprints are preliminary reports that have not undergone peer review.
They should not be considered conclusive, used to inform clinical practice,
or referenced by the media as validated information.

Functional Organization of the Endoplasmic Reticulum Dictates the Susceptibility of Target Cells to Arsenite-Induced Mitochondrial Superoxide Formation, Mitochondrial Dysfunction and Apoptosis

Andrea Guidarelli
University of Urbino
Alessia Catalani
University of Urbino
Ersilia Varone
Mario Negri Institute for Pharmacological Research
Stefano Fumagalli
Mario Negri Institute for Pharmacological Research
Ester Zito
Mario Negri Institute for Pharmacological Research
Mara Fiorani
University of Urbino
Orazio Cantoni (orazio.cantoni@uniurb.it)
University of Urbino
Andrea Spina
University of Urbino

Research Article

Keywords: arsenite, ryanodine receptor, inositol-1, 4, 5-triphosphate receptor, mitochondrial Ca2+, mitochondrial superoxide, mitochondrial permeability transition, apoptosis

Posted Date: May 13th, 2021

DOI: https://doi.org/10.21203/rs.3.rs-479781/v1

License: This work is licensed under a Creative Commons Attribution 4.0 International License.
Read Full License

Version of Record: A version of this preprint was published at Food and Chemical Toxicology on October 1st, 2021. See the published version at https://doi.org/10.1016/j.fct.2021.112523.

Functional organization of the endoplasmic reticulum dictates the susceptibility of target cells to arsenite-induced mitochondrial superoxide formation, mitochondrial dysfunction and apoptosis

Andrea Guidarelli[1], Alessia Catalani[1], Andrea Spina[1], Ersilia Varone[2], Stefano Fumagalli[2], Ester Zito[2], Mara Fiorani[1] and Orazio Cantoni[1]

[1]*Department of Biomolecular Sciences, University of Urbino Carlo Bo, Urbino, Italy.*

[2] *Istituto di Ricerche Farmacologiche Mario Negri IRCCS, Milan, Italy*

Corresponding author: Prof. Orazio Cantoni, Dipartimento di Scienze Biomolecolari, Sezione di Farmacologia e Farmacognosia, Università degli Studi di Urbino, Via S. Chiara 27, 61029 Urbino (PU), Italy. Tel: +39-0722-303523; Fax: +39-0722-305470; e-mail: orazio.cantoni@uniurb.it

Abstract

Arsenite induces many critical effects associated with the formation of reactive oxygen species (ROS) through different mechanisms. We focused on the Ca^{2+}-dependent mitochondrial superoxide ($mitoO_2^{-\cdot}$) formation and addressed questions on the effects of low concentrations of arsenite on the mobilization of the cation from the endoplasmic reticulum and the resulting mitochondrial accumulation. Using various differentiated and undifferentiated cell types uniquely expressing the inositol-1, 4, 5-triphosphate receptor (IP_3R), or both the IP_3R and the ryanodine receptor (RyR), we determined that expression of this second Ca^{2+} channel is an absolute requirement for $mitoO_2^{-\cdot}$ formation and for the ensuing mitochondrial dysfunction and downstream apoptosis. In arsenite-treated cells, RyR was recruited after IP_3R stimulation and agonist studies indicated that in these cells RyR is in close apposition with mitochondria. It was also interesting to observe that arsenite fails to promote mitochondrial Ca^{2+} accumulation, $mitoO_2^{-\cdot}$ formation, mitochondrial toxicity in RyR-devoid cells, in which the IP_3R is in close contact with the mitochondria. We therefore conclude that low dose arsenite-induced $mitoO_2^{-}$ formation and the resulting mitochondrial dysfunction and toxicity, are prerequisite of cell types expressing the RyR in close apposition with mitochondria.

Keywords: arsenite; ryanodine receptor; inositol-1, 4, 5-triphosphate receptor; mitochondrial Ca^{2+}; mitochondrial superoxide; mitochondrial permeability transition; apoptosis

Introduction

Arsenite is an important carcinogen and toxic compound (Flora 2011; Jomova et al. 2011; Minatel et al. 2018) that causes a plethora of effects in target cells, through its direct binding to some biomolecules (Chang et al. 2012; Shen et al. 2013) and/or *via* the intermediate formation of reactive oxygen species (ROS) (Flora 2011; Jomova et al. 2011; Hu et al. 2020). Given the relevance of this second event (Flora 2011; Jomova et al. 2011; Hu et al. 2020), it would be important to determine the mechanism whereby the metalloid promotes the formation of these species, to eventually establish a causal relationship with the effects generated in specific subcellular compartments. Indeed, short-lived species more likely generate relevant effects in the same sites of their formation, or in the close vicinity, thereby affecting the ensuing toxic response.

Unfortunately, the very large majority of the available studies provided a general indication of arsenite-induced ROS formation, with no systematic attempt to identify their origin, and thus the overall scenario remains poorly understood. The underlying mechanisms were investigated only in a few studies, which however demonstrated the involvement of either the mitochondrial respiratory chain (Liu et al. 2005; Guidarelli et al. 2020; Hu et al. 2020) or NADPH oxidase (Smith et al. 2001; Straub et al. 2008; Guidarelli et al. 2019a; Hu et al. 2020), but that nevertheless failed to provide a plausible explanation for these apparent discrepancies. Hence, arsenite potentially activates at least two important mechanisms of ROS formation, and the reasons of the prevalence of a mechanism over the other remain poorly understood.

It is interesting to note that in undifferentiated U937 (U-U937) cells, low concentrations of arsenite uniquely promote mitochondrial superoxide ($mitoO_2^{\cdot-}$) formation (Guidarelli et al. 2019a), *via* a mechanism requiring mitochondrial Ca^{2+} accumulation (Guidarelli et al. 2019b; Guidarelli et al. 2020). While the direct mitochondrial effects were maximally induced after a very short time of exposure, and with low dose requirements, much longer exposure and greater concentrations of the

metalloid were necessary to mobilize Ca^{2+} from the endoplasmic reticulum (ER) and promote the mitochondrial accumulation of the cation (Guidarelli et al. 2020).

More specifically, arsenite promotes an initial slow mobilization of a limited amount of Ca^{2+} from the inositol-1, 4, 5-triphosphate receptor (IP_3R), critical for the triggering of an intraluminal crosstalk between the IP_3R and the ryanodine receptor (RyR), leading to further release of large amounts of Ca^{2+} (Guidarelli et al. 2018). Interestingly, only the fraction of Ca^{2+}derived from the RyR was taken up by the mitochondria, as demonstrated by experiments using RyR antagonists as well as differentiated U937 cells (D-U937), failing to express functional RyR (Guidarelli et al. 2009; Guidarelli et al. 2018). In addition, RyR was also the source of Ca^{2+} accumulating in mitochondria after stimulation with IP_3 releasing agonists (Clementi et al. 1998; Guidarelli et al. 2020), thereby providing indirect experimental evidence for a close spatial and functional connection between the RyR and mitochondria of the cell line employed in our experiments (Guidarelli et al. 2019b; Guidarelli et al. 2020).

From the above findings, we can formulate a hypothesis for the mechanism whereby arsenite promotes mito$O_2^{-\cdot}$ formation in U-U937 cells, based on the spatial and functional organization of their ER, in particular on the reciprocal topology of the two Ca^{2+} release receptors, the IP_3R and RyR, and their relative vicinity to mitochondria. It is indeed well established that contact sites between the ER and mitochondria regulate Ca^{2+} transfer between these two organelles, through the low affinity mitochondrial Ca^{2+} uniporter (MCU) (Kirichok et al. 2004; Rizzuto et al. 2012), which requires cytosolic Ca^{2+} concentrations ($[Ca^{2+}]_c$ in the 10-20 μM range. These high $[Ca^{2+}]_c$ can be reached only in the very close proximity of the IP_3R or the RyR, when activated by agonist stimulation, or treatment with toxic compounds (Van Petegem 2012; Bansaghi et al. 2014; Berridge 2016; Guidarelli et al. 2019b)

The aforementioned hypothesis initially build up on experiments performed in U-U937 and their respiration-deficient counterpart, as well as in D-U937, can be challenged in other cell types

characterised by a different spatial organization of the ER, to pinpoint a unique critical mechanism for arsenite-induced mito$O_2^{-\cdot}$ formation, and hence for the resulting downstream events, which include mitochondrial dysfunction and mitochondrial permeability transition (MPT)-dependent apoptotic death (Guidarelli et al. 2019b).

In this study, we aim to investigate whether arsenite-induced mitoO_2^- formation, and the ensuing MPT-dependent mitochondrial toxicity, is a prerogative of cell types with functional interactions between the IP_3R and the RyR, with this second channel in close apposition with mitochondria. Furthermore, we also investigate whether the metalloid promotes mitochondrial Ca^{2+} accumulation and mitoO_2^- formation in cells that do not express the RyR, in which the IP_3R is in fact in close contact with the mitochondria.

Results

Characteristics of the experimental cell types

In this study, we used U-U937 cells, which express both IP_3R and RyR (Sugiyama et al. 1994; Clementi et al. 1998; Hosoi et al. 2001; Guidarelli et al. 2009), that can be differentiated to monocytes (D-U937) with concomitant downregulation of the RyR (Guidarelli et al. 2009). This versatile cellular model leads to assess the relative impact of the IP_3R in a cellular environment with RyR presence or deficiency and in conditions respectively of proliferation (U-U937) or non-proliferation (D-U937). We also included in our experimental setting a different cell type that instead gains RyR expression following differentiation, i.e. C2C12 cells. Indeed, C2C12 myoblasts (U-C2C12) express only IP_3R (Bennett et al. 1996; Tarroni et al. 1997), whereas C2C12 myotubes (D-C2C12) express a functional RyR too (Airey et al. 1991; Bennett et al. 1996; Tarroni et al. 1997). We exploit also HeLa cells, which express IP_3R but not RyR ((Bennett et al. 1996) and see below). In summary, this study involved the use of: i) three cell types expressing only IP_3R, two of which were proliferating (HeLa and U-C2C12 cells) and the third one non-proliferating (D-U937 cells); ii) two cell types expressing both IP_3R and RyR, i.e., U-U937 cells (proliferating) and D-C2C12 cells (non-proliferating).

Arsenite-induced Ca^{2+} response depends on RyR function

We exploit agonist studies to provide functional evidence of IP_3R and RyR activity in different cell lines. Logarithmically growing HeLa cells were exposed for 10 min to 10 mM Cf, an agonist of the RyR (Meissner 2017), and the $[Ca^{2+}]_c$ was determined. The results shown in Fig. 1a indicate that Cf fails to promote an increase in the $[Ca^{2+}]_c$ of these cells, as it also happens in D-U937 or U-C2C12 cells, i.e., other cell types devoid of RyR (Bennett et al. 1996; Tarroni et al. 1997; Guidarelli et al. 2009).

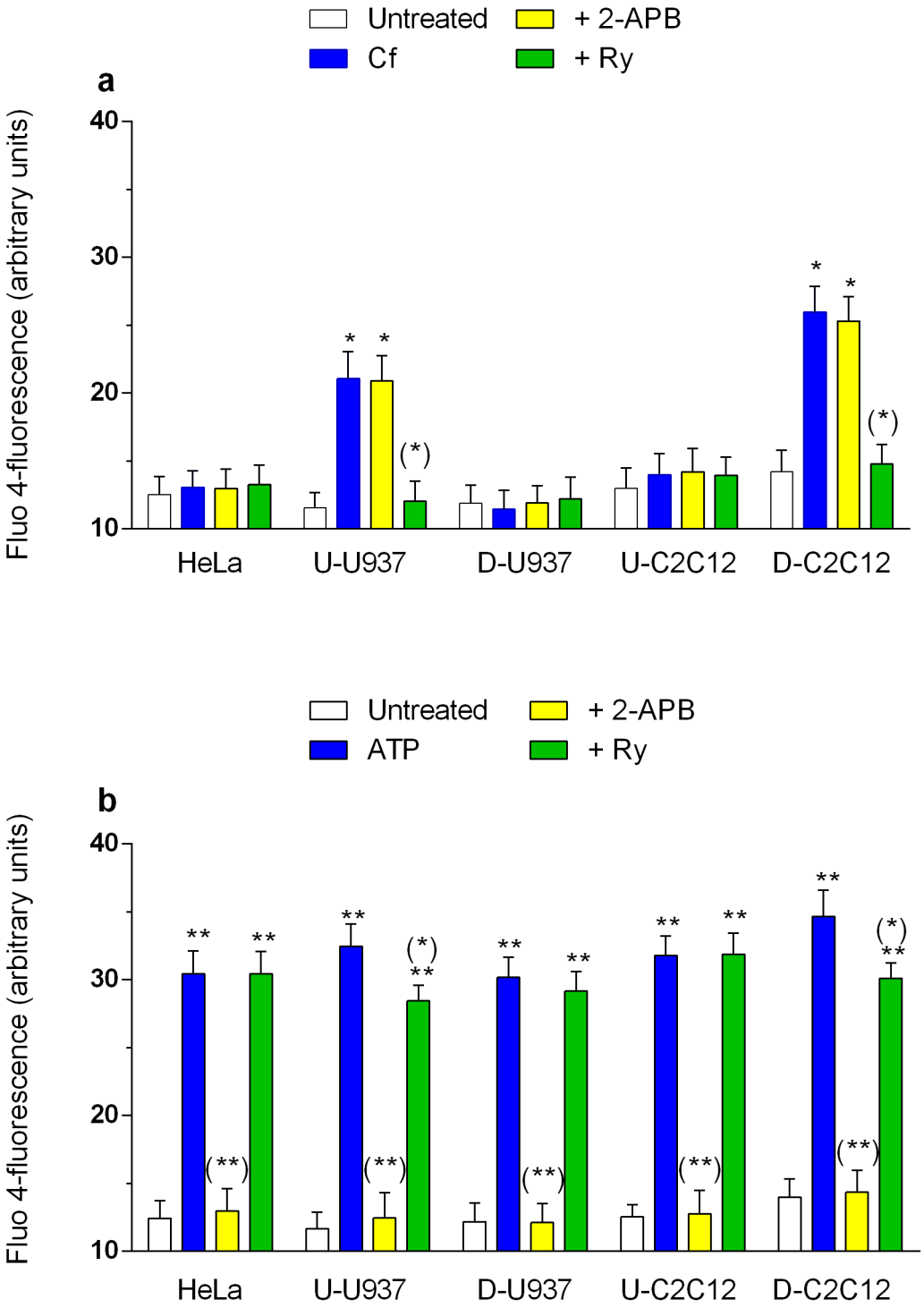
Untreated
+ 2-APB
Cf
+ Ry
a
Fluo 4-fluorescence (arbitrary units)
40
30
20
10
HeLa
U-U937
D-U937
U-C2C12
D-C2C12
Untreated
+ 2-APB
ATP
+ Ry
b
Fluo 4-fluorescence (arbitrary units)
40
30
20
10
HeLa
U-U937
D-U937
U-C2C12
D-C2C12

Fig. 1

In contrast, a significant Ca^{2+} response, sensitive to 20 μM Ry (a RyR antagonist, (Van Petegem 2012; Meissner 2017)), and insensitive to 50 μM 2-APB (an IP_3R antagonist, (Berridge 2016)), was detected in U-U937-cells and D-C2C12 cells, i.e., cell types with a functional RyR (Fig. 1a). Some experiments were also performed by replacing Cf with 4-chloro-m-cresol (300 μM), another RyR agonist (Van Petegem 2012), with identical outcomes (not shown).

We next tested the effect of 100 μM ATP (for 10 min), an agonist of GQ-protein-linked receptors leading to Ca^{2+} mobilization from the IP_3R (Berridge 1993). In HeLa, U-C2C12 and D-U937 cells, ATP caused a significant increase of $[Ca^{2+}]_c$, sensitive to 2-APB and insensitive to Ry (Fig. 1b). The Ca^{2+} response mediated by ATP in U-U937 or D-C2C12 cells, besides being sensitive to 2-APB, was partially blunted by Ry in a statistically significant manner.

Altogether, these results are therefore in line with the notion that HeLa, U-C2C12 and D-U937 cells, unlike U-U937 cells or D-C2C12 cells, do not have a functional RyR. IP_3R was instead responsive to agonist stimulation in all of these five cell types. U-U937 or D-C2C12 cells responded to the IP_3-generating agonist with the release of Ca^{2+} from the IP_3R together with an additional aliquot of the cation from the RyR.

After this initial characterization of the aforementioned cell lines with IP_3R and RyR agonists, we tested the effects of a 6 h exposure to a 2.5 μM concentration of arsenite, as previously done in U-U937 cells. This treatment was devoid of intrinsic toxic effects in all cell types, as determined by the trypan blue assay (which detects loss of plasma membrane integrity) and the Hoechst assay (which detects apoptotic DNA fragmentation and condensation) (Supplementary Fig. 1).

We then found that, under identical conditions, arsenite caused a limited increase in $[Ca^{2+}]_c$ in HeLa, U-C2C12 and D-U937 cells, invariably sensitive to 2-APB and insensitive to Ry (Fig. 2a).

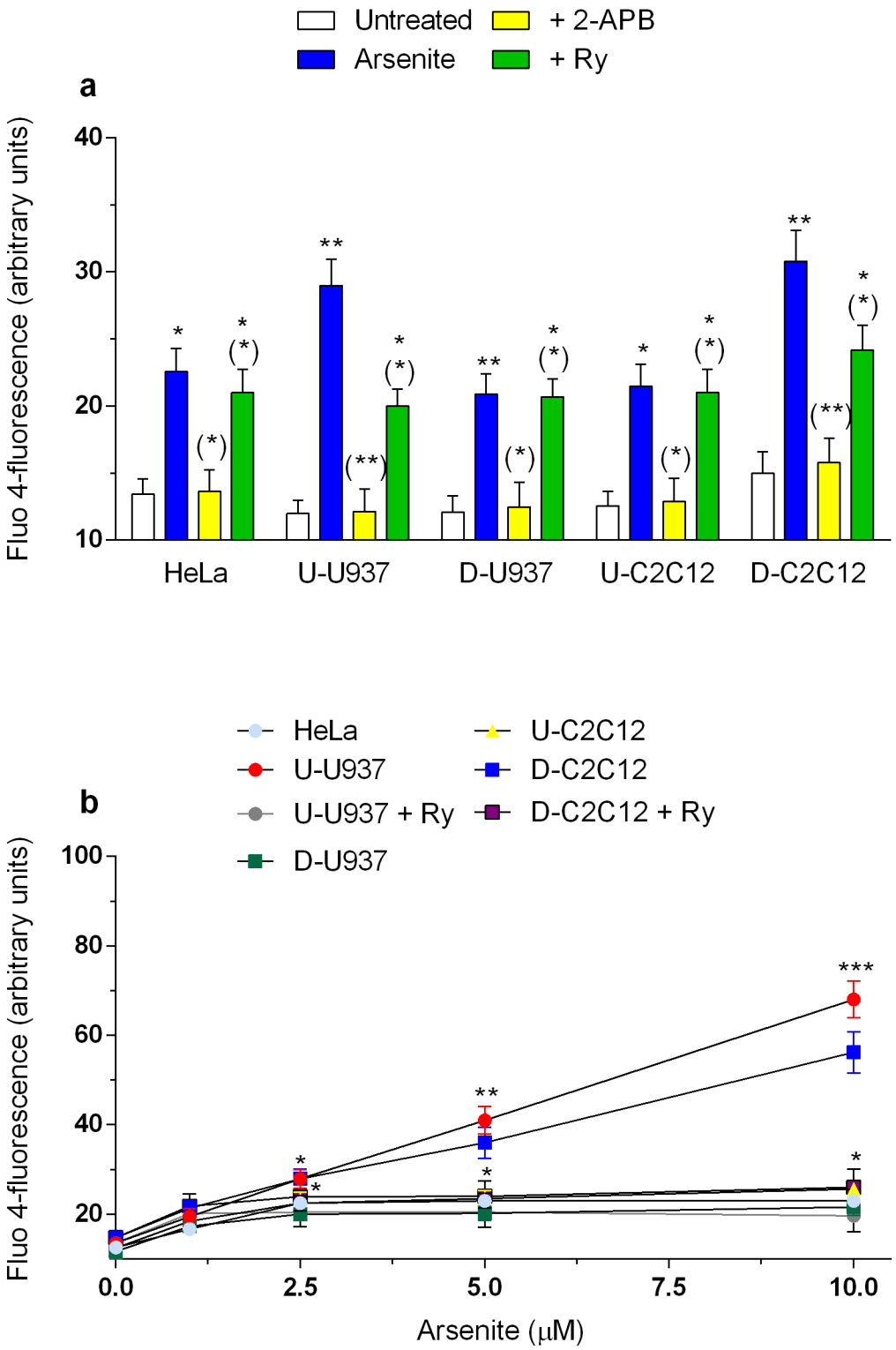
a
Untreated
+ 2-APB
Arsenite
+ Ry
Fluo 4-fluorescence (arbitrary units)
40
30
20
10
HeLa
U-U937
D-U937
U-C2C12
D-C2C12
b
HeLa
U-U937
U-U937 + Ry
D-U937
U-C2C12
D-C2C12
D-C2C12 + Ry
Fluo 4-fluorescence (arbitrary units)
100
80
60
40
20
0.0
2.5
5.0
7.5
10.0
Arsenite (μM)

Fig. 2

The Ca^{2+} response induced by the metalloid in U-U937, or D-C2C12, cells was instead significantly greater, abolished by 2-APB and remarkably reduced by Ry. It is interesting to note that the $[Ca^{2+}]_c$ of U-U937 or D-C2C12 cells supplemented with arsenite and Ry were quantitatively identical to those detected in D-U937, U-C2C12 and HeLa cells treated with the metalloid alone.

We next investigated the arsenite concentration-dependence on the $[Ca^{2+}]_c$ and obtained evidence for a saturable mechanism in HeLa, D-U937 and U-C2C12 cells (Fig. 2b). More specifically, the release of the cation from the IP_3R was maximally stimulated by 2.5 μM arsenite, whereas in U-U937 or D-C2C12 cells the effects of the metalloid were concentration-dependent within the tested concentration range, i.e., 2.5-10 μM. Importantly Ry, by preventing Ca^{2+} release from the RyR, normalized the Ca^{2+} response of U-U937 cells to that of D-U937 cells, and the response of D-C2C12 cells to that of U-C2C12 cells. In addition, all these responses were quantitatively similar to that of HeLa cells.

Arsenite, therefore, stimulates the release of Ca^{2+} from the IP_3R in different cell types, regardless of the structural/functional organization of the ER and of their differentiation state. The Ca^{2+} response mediated *via* IP_3R activation, while limited and saturable, is significantly and dose-dependently increased in RyR-expressing cells, once again regardless of their differentiation state.

Arsenite fails to increase the mitochondrial concentration of Ca^{2+} in cells exclusively expressing the IP_3R

We initially determined the mitochondrial clearance of Ca^{2+} in the aforementioned five cell types. The IP_3 releasing agonist significantly increased the $[Ca^{2+}]_m$ in HeLa (Fig. 3a), D-U937 cells (Fig. 3c) and U-C2C12 (Fig. 3d), *via* a mechanism sensitive to 10 μM Ru360 (a MCU inhibitor, (Zazueta et al. 1999)), or 2-APB, but insensitive to Ry.

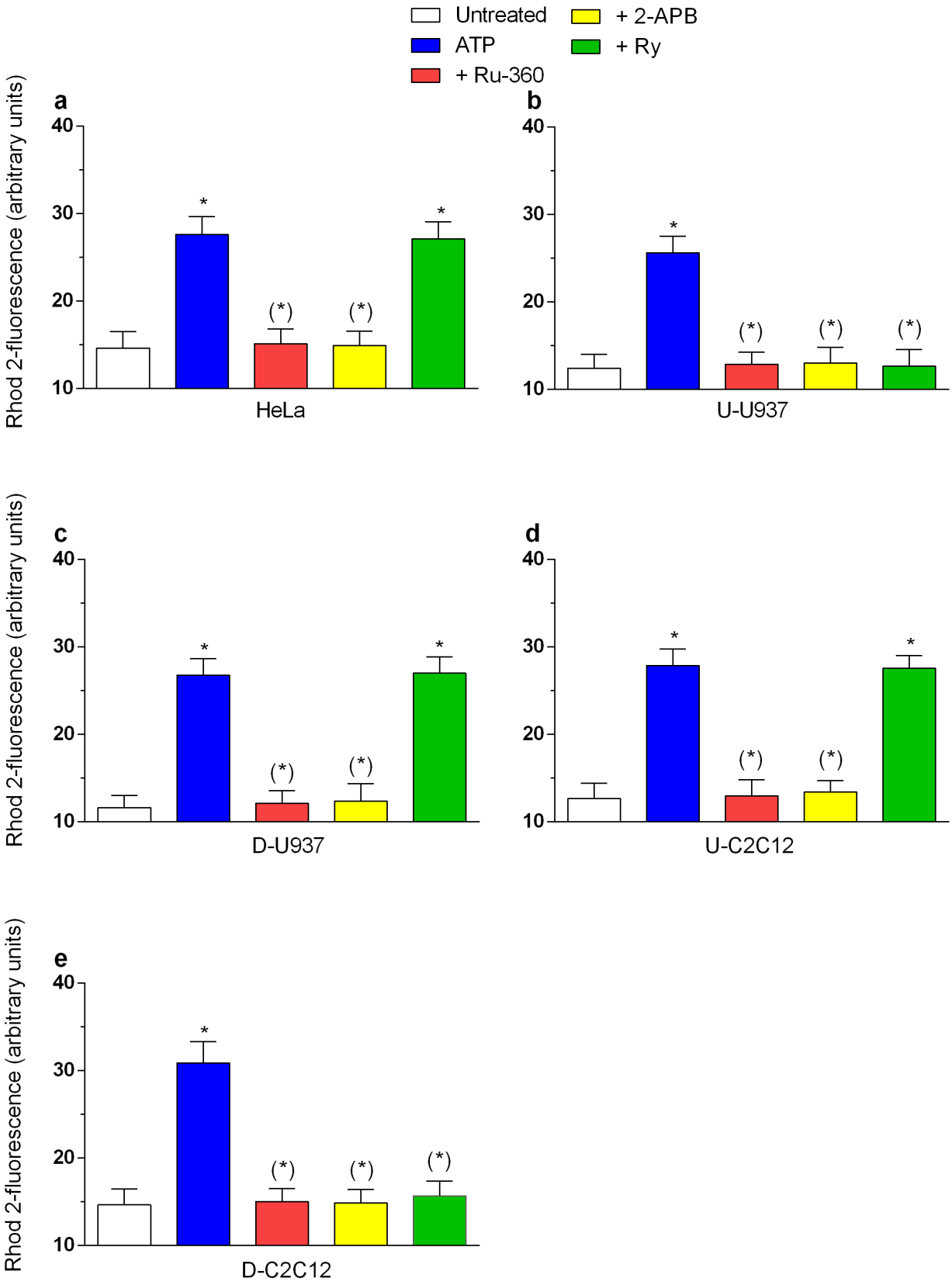
Untreated
ATP
+ Ru-360
+ 2-APB
+ Ry
a
b
c
d
e
Rhod 2-fluorescence (arbitrary units)
HeLa
U-U937
D-U937
U-C2C12
D-C2C12
10
20
30
40
*
(*)

Fig. 3

Experiments performed in U-U937 (Fig. 3b) and D-C2C12 (Fig. 3e) cells provided outcomes in line with the notion that ATP leads to increased $[Ca^{2+}]_m$ that, besides being sensitive to Ru360, or 2-APB, is also suppressed by Ry. The effects mediated by Ry in U-U937 or D-C2C12 cells were consistent with the results obtained in D-U937 or U-C2C12 cells, respectively.

Therefore, these findings suggest that an IP_3 releasing agonist induces mitochondrial Ca^{2+} accumulation in cells that do not express the RyR. Instead, in RyR expressing cells, the IP_3 releasing agonist induces mitochondrial Ca^{2+} accumulation *via* the intermediate action of the RyR.

We next addressed the question of whether arsenite promotes mitochondrial Ca^{2+} accumulation in cells exclusively expressing the IP_3R. A 6 h exposure to arsenite (2.5 μM) triggered a maximal response in terms of Ca^{2+} release from IP_3R (Fig. 2b) but failed to increase $[Ca^{2+}]_m$ in HeLa (Fig. 4a), D-U937 (Fig. 4c) and U-C2C12 cells (Fig. 4d). We instead observed a significant mitochondrial Ca^{2+} signal in U-U937 cells (Fig. 4b) and D-C2C12 cells (Fig. 4e), in both circumstances sensitive to Ru360, 2-APB and Ry. Furthermore, greater concentrations of arsenite failing to promote detectable responses in HeLa, D-U937 and U-C2C12 cells, caused a concentration-dependent mitochondrial uptake of the cation in U-U937 and D-C2C12 cells (Fig. 4 f).

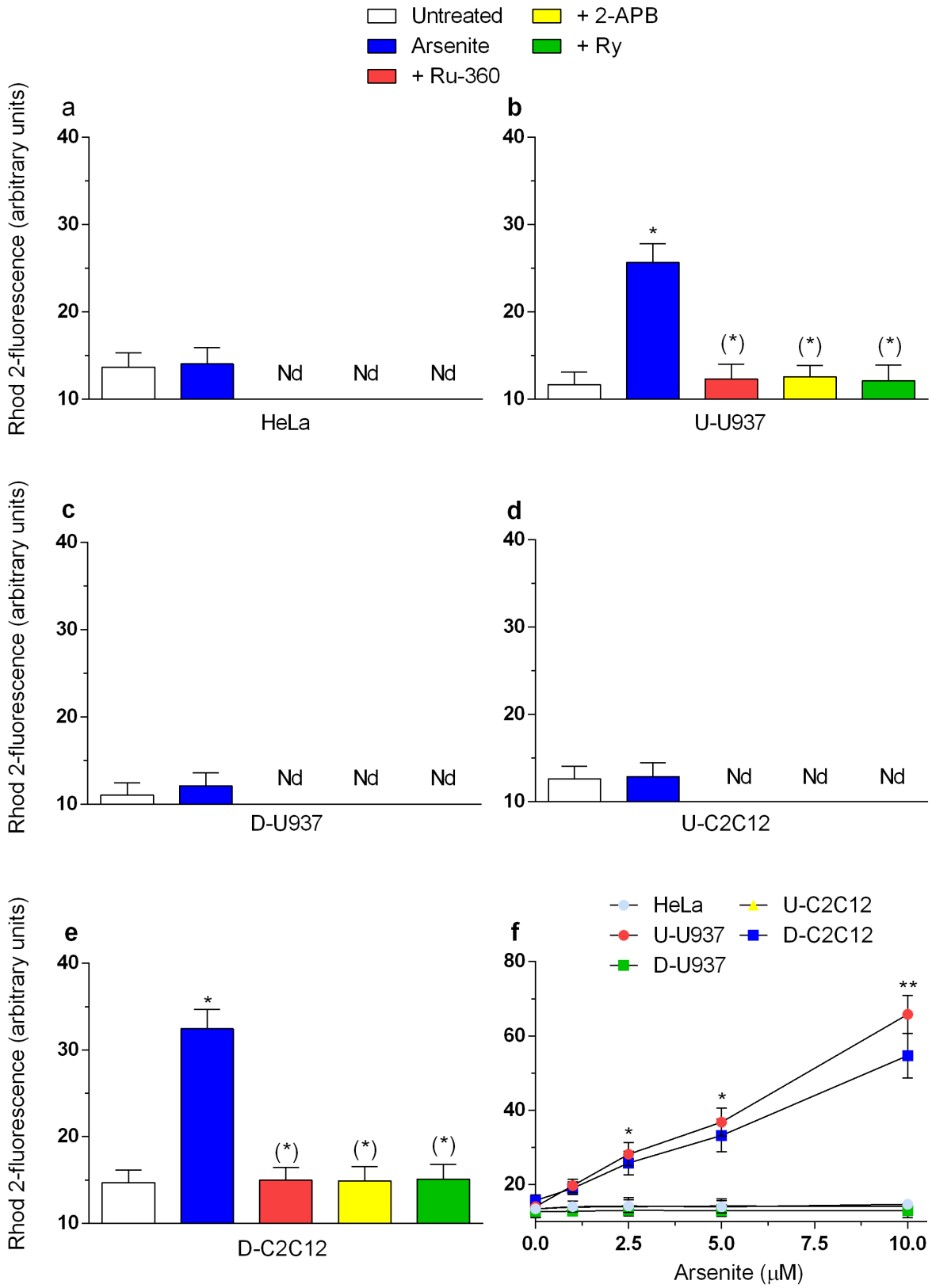
Untreated
Arsenite
+ Ru-360
+ 2-APB
+ Ry
a
b
c
d
e
f
Rhod 2-fluorescence (arbitrary units)
HeLa
U-U937
D-U937
U-C2C12
D-C2C12
Nd
(*)
*
**
Arsenite (μM)

Fig. 4

Confocal and SIM microscopy also corroborated by the quantitative Manders coefficient confirmed that 2.5 µM arsenite raises Rhod-2AM fluorescence in mitochondria, hence mitochondrial Ca^{2+} of D-C2C12 (Fig.4 g-i) and of U-U937 (not shown).

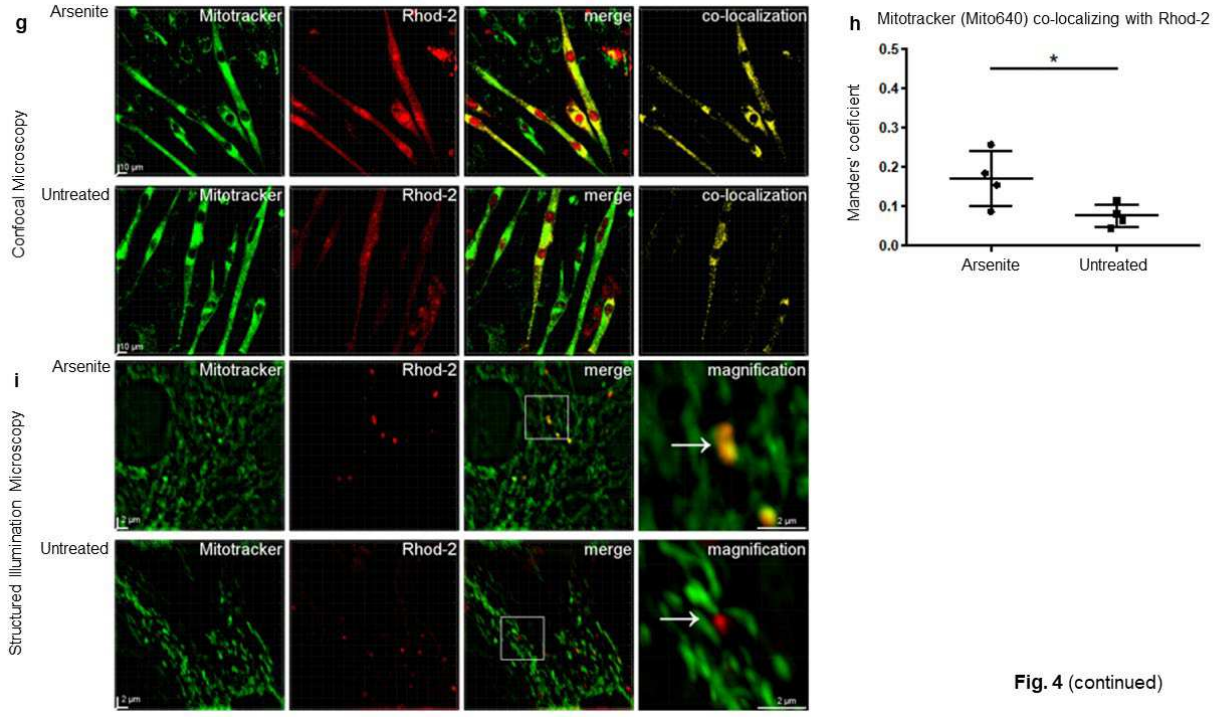

Fig. 4 (continued)

These results therefore indicate that, in cells uniquely expressing the IP_3R, mitochondrial Ca^{2+} accumulation ensues after treatment with a IP_3 releasing agonists, but not with arsenite. IP_3R stimulation with either of these treatments instead increased the $[Ca^{2+}]_m$ in RyR expressing cells, in which RyR is in close contact with the mitochondria.

Arsenite does not trigger mito$O_2^{\cdot-}$ in cells with the only IP_3R

The cells were exposed for 6 h to 2.5 µM arsenite and analyzed for ROS formation using DHR (Gomes et al. 2005). This probe is not taken up by the mitochondria but is susceptible to oxidation by the H_2O_2 released from these organelles after dismutation of mito$O_2^{\cdot-}$ by Mn superoxide dismutase (Weisiger et al. 1973). In addition, $O_2^{\cdot-}$ formation can also take place in the mitochondrial intermembrane space upon interaction of electrons released by complex III with molecular oxygen, with its subsequent conversion to H_2O_2 catalysed by Cu/Zn superoxide dismutase (Angelova et al.

2016). DHR is therefore a sensitive marker of $O_2^{\cdot -}$ formation generated in both the mitochondrial and extra mitochondrial compartments.

In other experiments, DHR was replaced with MitoSOX red, a fluorochrome commonly employed for the detection of $O_2^{\cdot -}$ in the mitochondria of live cells (Mukhopadhyay et al. 2007).

The results illustrated in Fig 5 indicate that HeLa (a and b), D-U937 (e and f) or U-C2C12 (g and h) cells fail to respond to arsenite with detectable fluorescent signals, instead readily observed in U-U937 (c and d) or D-C2C12 (i and j) cells. The results obtained in the latter two cell types are indicative of Ca^{2+}-dependent mito$O_2^{\cdot -}$ formation, a notion consistent with the observation that Ru360, 2-APB and Ry suppress the arsenite-induced fluorescence responses (c and d as well as i and j), under the same conditions in which these agents also blunted mitochondrial Ca^{2+} accumulation (Fig. 4b and e).

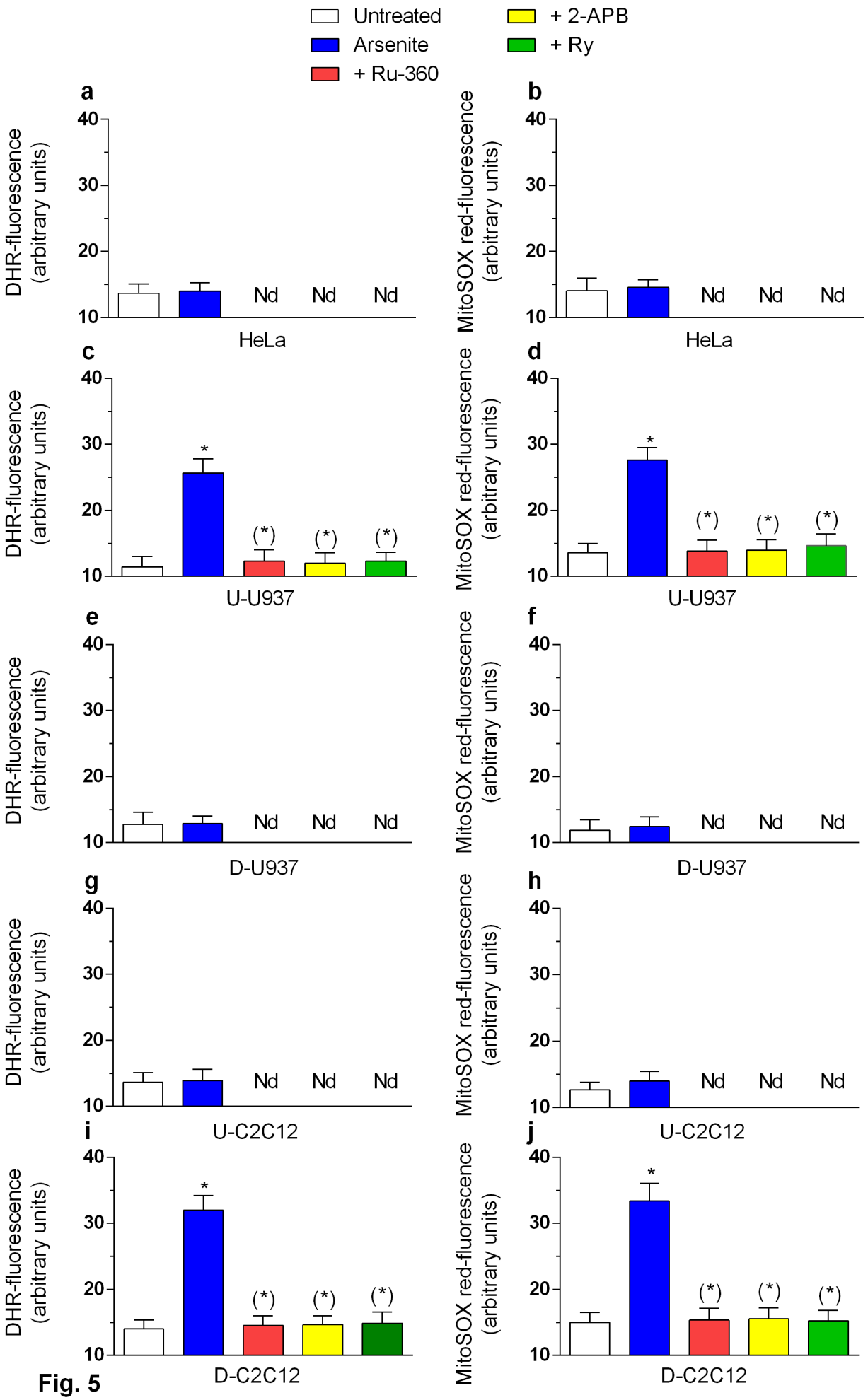
Untreated
Arsenite
+ Ru-360
+ 2-APB
+ Ry
a
b
c
d
e
f
g
h
i
j
DHR-fluorescence (arbitrary units)
MitoSOX red-fluorescence (arbitrary units)
40
30
20
10
Nd
Nd
Nd
*
(*)
(*)
(*)
HeLa
U-U937
D-U937
U-C2C12
D-C2C12

Fig. 5

It is interesting to note that qualitatively identical results were obtained with DHR and MitoSOX red, thereby implying that, under the conditions employed, arsenite uniquely induces Ca^{2+}-dependent $mitoO_2^{-\cdot}$ formation in responsive RyR-expressing cells.

We finally asked the question of whether the resistance of HeLa, D-U937 and U-C2C12 cells to $mitoO_2^{-\cdot}$ formation induced by arsenite is uniquely dependent on the lack of mitochondrial Ca^{2+} accumulation. For this purpose, we reasoned that this phenotype should be lost under conditions in which the mitochondrial accumulation of Ca^{2+} is enforced by other treatments. In this perspective, ATP represents an excellent tool to increase the $[Ca^{2+}]_m$ in HeLa, U-C2C12 and D-U937 cells, as detailed in the above characterization studies (Fig. 3a, c and d). We therefore performed experiments in which the cells were supplemented with ATP in the last 10 min of the 6 h incubation in an arsenite-containing medium. As indicated in Fig. 6, the arsenite/ATP regimen caused a significant, Ru360 and 2-APB-sensitive, albeit Ry-insensitive, MitoSOX red fluorescence response in each of the three different cell lines. Note that arsenite alone, as also discussed above, fails to increase the $[Ca^{2+}]_m$ and to promote $mitoO_2^{-\cdot}$ formation in the absence of additional treatments.

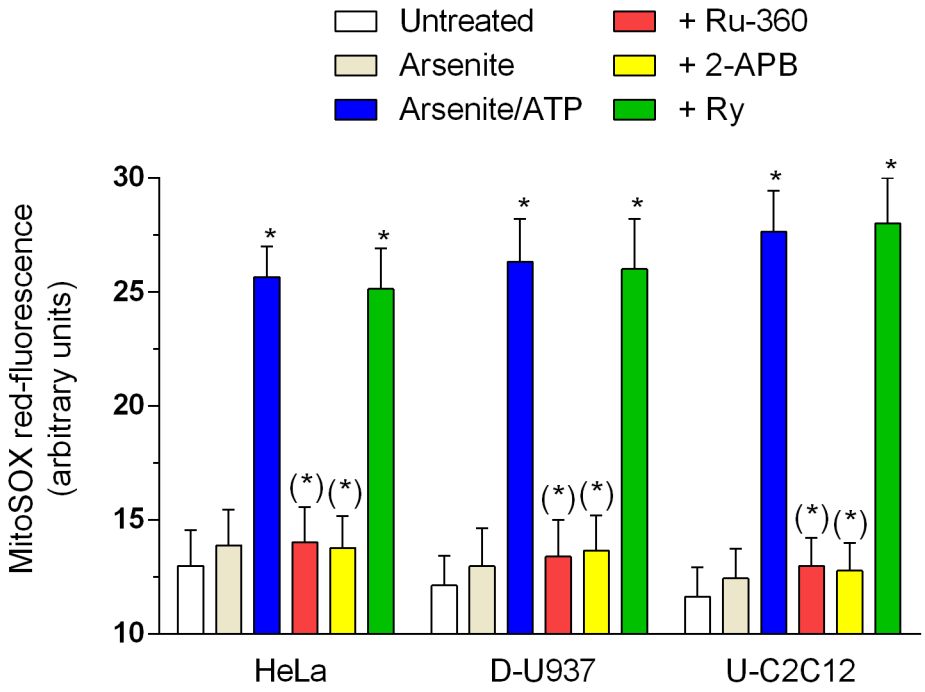
Untreated
Arsenite
Arsenite/ATP
+ Ru-360
+ 2-APB
+ Ry
MitoSOX red-fluorescence
(arbitrary units)
30
25
20
15
10
*
(*)
HeLa
D-U937
U-C2C12

Fig. 6

These results therefore indicate that arsenite fails to promote mito$O_2^{-\cdot}$ formation in cells devoid of RyR for the only reason that they are unable to respond to the metalloid with a significant increase in the $[Ca^{2+}]_m$.

Arsenite induces mitochondrial toxicity in RyR expressing cells

We recently reported that exposure to 2.5 μM arsenite promotes mito$O_2^{-\cdot}$-dependent mitochondrial dysfunction and apoptosis in U-U937 (Guidarelli et al. 2019b). Consistently, we observe that a 16 h exposure to arsenite causes (Fig. 7b) a decrease of mitochondrial membrane potential (i) and a significant mitochondrial loss of cytochrome c (ii). In addition, after a further 8 h of incubation, there was evidence of caspase 3 activation (iii), loss of MTT-reducing activity (iv), reduced rate of proliferation (v) and increased apoptotic DNA fragmentation (vi). It was then interesting to observe that these results are in qualitative agreement with those obtained using D-C2C12 cells (Fig. 7e, i-iv and vi), with however an expected difference in cell proliferation experiments (v). D-C2C12 cells are non-proliferating cells and thus their number remained unchanged after exposure to arsenite.

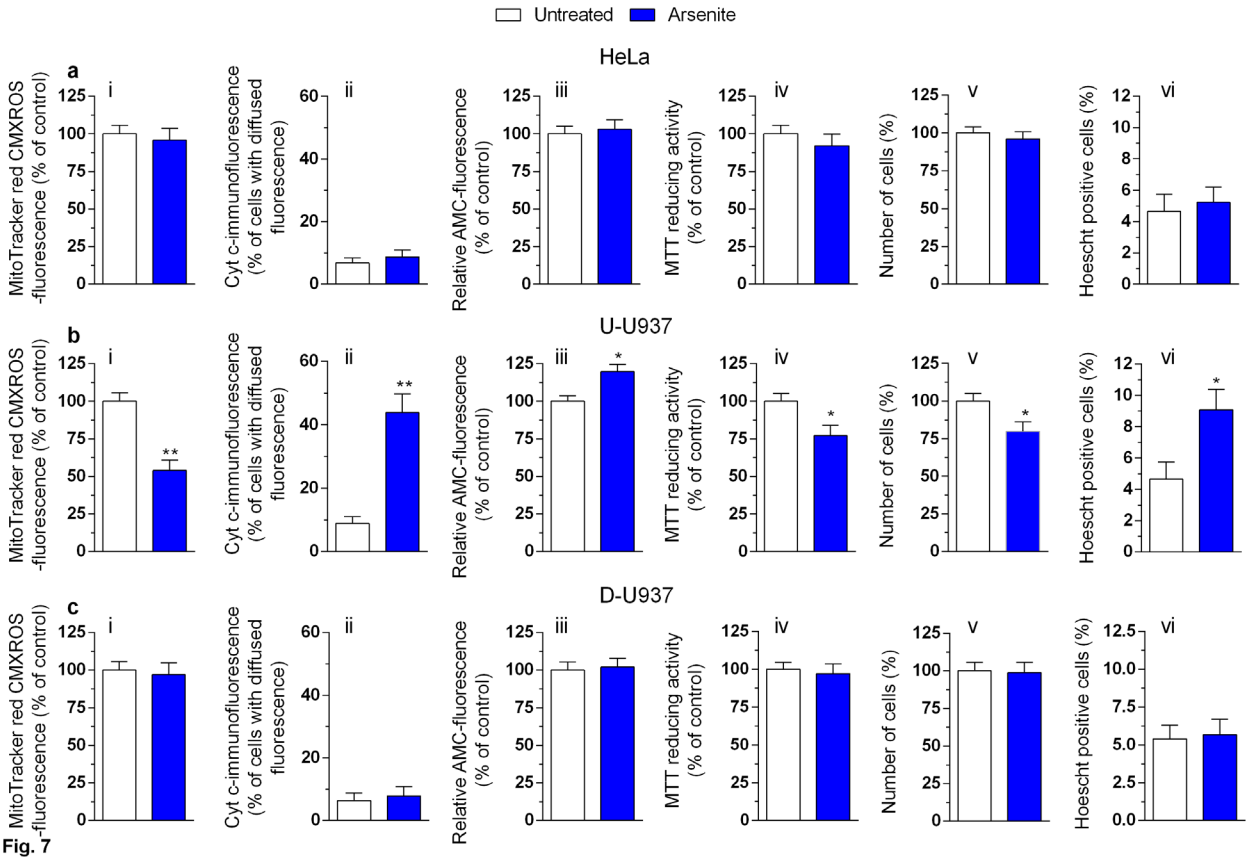

Fig. 7

Experiments performed in HeLa (Fig. 7a), D-U937 (Fig. 7c) and U-C2C12 (Fig. 7d), devoid of RyR, and hence resistant to mito$O_2^{\cdot-}$ formation, provided evidence for a parallel resistance to mitochondrial dysfunction and cytotoxicity induced by arsenite. More specifically, in these cells, there was no evidence for a decrease in mitochondrial membrane potential (i), mitochondrial loss of cytochrome c (ii), caspase 3 activation (iii) or apoptotic DNA fragmentation (vi). In addition, arsenite did not affect the proliferation rates of HeLa (Fig. 7av) and U-C2C12 (Fig. 7dv) whereas the number of D-U937 cells (Fig. 7cv), i.e., non-proliferating monocytes, remained unchanged after the 24 h arsenite treatment.

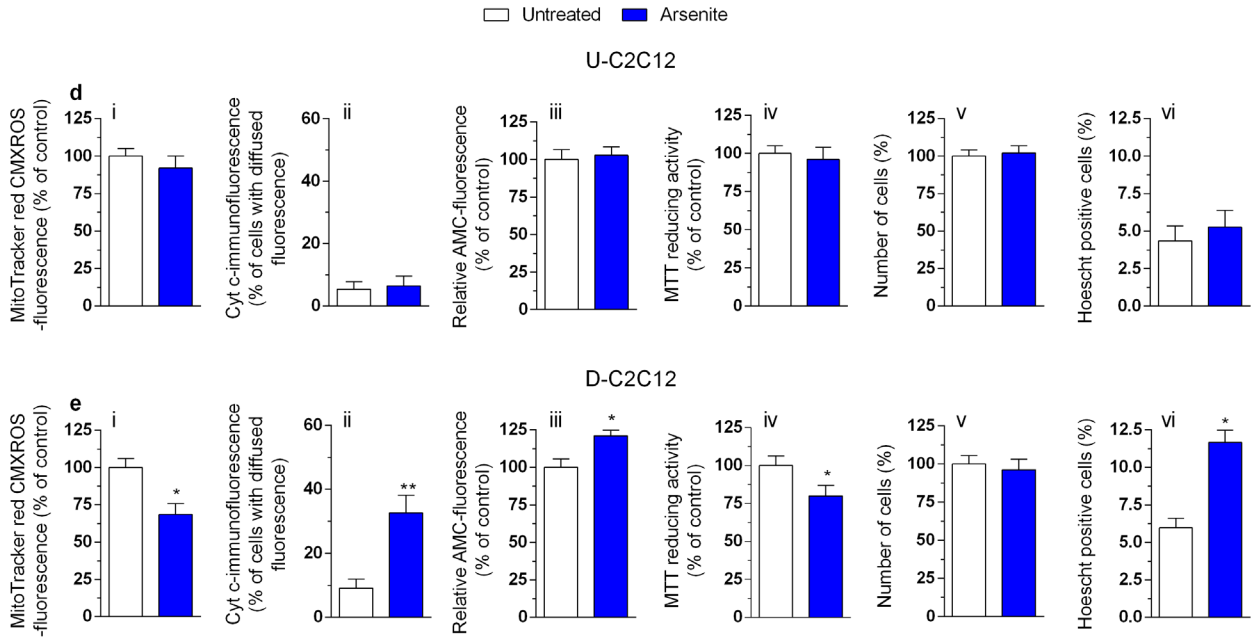

Fig. 7 (continued)

These results indicate that arsenite exposure triggers mitochondrial toxicity in proliferating and non-proliferating RyR expressing cells, permissive for mito$O_2^{\cdot-}$ formation. Cells exclusively expressing the IP_3R, were instead resistant to arsenite-induced mitochondrial ROS formation and to the ensuing mitochondrial toxicity.

Discussion

Under physiological conditions, specific extracellular signals transiently increase the $[Ca^{2+}]_c$ and subsequently the $[Ca^{2+}]_m$ to stimulate oxidative phosphorylation and other mitochondrial events (Denton 2009; Bhosale et al. 2015). This sequence of events likely takes place after IP_3-generating agonist stimulation of HeLa, D-U937 cells and U-C2C12 cells, as the IP_3R they express in the absence of RyR apparently generates high $[Ca^{2+}]_c$ in mitochondrial microdomains in which MCU-dependent transport of the cation readily ensues. Hence, D-U937 cells have a different functional organization of the ER/mitochondria network in comparison with their undifferentiated counterpart, as the Ca^{2+} mobilized from U-U937 cells *via* IP_3Rs caused mitochondrial Ca^{2+} accumulation with the intermediate involvement of the RyR (Clementi et al. 1998; Guidarelli et al. 2020). D-C2C12 cells had a similar functional organization of U-U937 cells, as U-C2C12 cells gained expression of functional RyR during differentiation (Airey et al. 1991; Bennett et al. 1996; Tarroni et al. 1997). Given these findings, inhibition of Ca^{2+} release form the RyR of U-U937 or D-C2C12 cells, blunted or abolished the effects mediated by IP_3R stimulation on $[Ca^{2+}]_c$ or $[Ca^{2+}]_m$, respectively. As a final note, direct RyR stimulation with a high concentration of Cf increased both the $[Ca^{2+}]_c$ and $[Ca^{2+}]_m$ in U-U937 or D-C2C12 cells, and failed to produce effects in HeLa, D-U937 or U-C2C12 cells.

These results are therefore consistent with the notion that the differentiation process converts U-U937 cells, characterized by close contact sites between the RyR and mitochondria, to D-U937 cells, in which RyR down-regulation takes place in parallel with the formation of new contact sites between the IP_3R and the mitochondria, similar to those detected in HeLa cells. Specular changes instead ensue in the C2C12 cell line, which gained RyR expression with differentiation, thereby emphasizing the notion that the functional organization of ER is independent on events related to cell proliferation and/or differentiation.

This initial characterization provided critical information to ask specific questions on the mechanism whereby arsenite induces mitochondrial Ca^{2+} accumulation and $O_2^{-\cdot}$ formation.

We found that cells with IP_3R but devoid of RyR respond to the metalloid with a saturable and limited Ca^{2+} release, that failed to increase the $[Ca^{2+}]_m$ for reasons that remain at the moment poorly understood. However, previous studies performed in D-U937 cells, or in Ry-supplemented U-U937 cells, indicated that arsenite does not impair the Ca^{2+} response induced by ATP (Guidarelli et al. 2018), thereby suggesting that the possibility of an inhibitory effect on the IP_3R downstream signaling is unlikely. It is instead conceivable that the metalloid promotes a slow efflux of the cation from IP_3R, resulting in low $[Ca^{2+}]$ in microdomains sensed by the mitochondria, so that the cation is not efficiently transported in these organelles.

Our previous studies demonstrated that arsenite induces $mitoO_2^{-\cdot}$ formation *via* a Ca^{2+}-dependent process, since ROS emission was inhibited by various manipulations preventing the mitochondrial accumulation of the cation (Guidarelli et al. 2019b; Guidarelli et al. 2020). Hence, a direct consequence of the lack of mitochondrial Ca^{2+} accumulation was that arsenite fails to promote $mitoO_2^{-\cdot}$ formation in HeLa, D-U937 and U-C2C12 cells, that have only the IP_3R. The notion that the resistance phenotype of these cells is uniquely due to an insufficient $[Ca^{2+}]_m$ was further established by demonstrating their ability to generate $mitoO_2^{-\cdot}$ in response to arsenite, under conditions in which the mitochondrial accumulation of Ca^{2+} is enforced by an IP_3-releasing agonist. Thus, the mitochondrial respiratory chain of these cells is as susceptible as that of RyR expressing cells to arsenite, and indeed their inability to generate $mitoO_2^{-\cdot}$ appears to be uniquely dependent of their specific functional organization of the ER.

The scenario was remarkably different in cells expressing both the IP_3R and RyR, i.e. U-U937 and D-C2C12 cells, which responded to arsenite with a concentration-dependent increase in the $[Ca^{2+}]_c$ and, most importantly, the $[Ca^{2+}]_m$. RyR recruitment, after the initial IP_3R stimulation, was essential for both responses and for the resulting ability to generate $mitoO_2^{-\cdot}$, even at low concentrations of the metalloid.

Based on previous reports (Guidarelli et al. 2019b; Guidarelli et al. 2020), indicating that mito$O_2^{-\cdot}$ mediates mitochondrial dysfunction and delayed, caspase 3-dependent apoptotic death in U-U937 cells exposed to arsenite, we predicted that an identical sequence of events should take place in other RyR expressing cells, but not in cell types uniquely expressing the IP_3R. This notion was experimentally established, and indeed D-C2C12 turned out to be as sensitive as U-U937 cells to arsenite toxicity, whereas, under the same conditions, HeLa, D-U937 and U-C2C12 cells remained viable.

These and the above results are therefore in line with the notion that concomitant expression of functional IP_3R and RyR is required to respond to arsenite with an enhanced $[Ca^{2+}]_m$, mitoO_2-. formation, mitochondrial damage and the ensuing triggering of the mitochondrial pathway of apoptosis. In addition, the initial effects on Ca^{2+} homeostasis, as well as the entire sequence of downstream events, appeared independent on the proliferative and/or differentiation status of the cells.

The same low arsenite concentrations failing to promote mito$O_2^{-\cdot}$ formation, mitochondrial damage and the ensuing toxicity in cells uniquely expressing the IP_3R also failed to generate extra-mitochondrial ROS. We should however keep in mind that a resistance phenotype to a specific mechanism of ROS formation does not rule out the possibility of the recruitment of a second mechanism, e.g., NADPH oxidase activation, at increasing concentrations of the metalloid. Under these conditions, a MPT-independent mechanism of arsenite toxicity may eventually take place, due to the lack of mitochondrial Ca^{2+} accumulation and mitochondrial ROS formation. This notion is consistent with the outcome of a recent study (Guidarelli et al. 2019a) in which we provided evidence of NADPH oxidase activation and ROS formation in respiration-deficient U937 cells exposed to arsenite concentrations greater than 5 μM. It is also interesting to note that these conditions were associated with increased mitochondrial Ca^{2+} accumulation in the absence of mito$O_2^{-\cdot}$ formation.

In conclusion, the results presented in this study are in line with the concept that the spatial and functional organization of the ER dictates the susceptibility of specific cell types to arsenite-induced mitochondrial Ca^{2+} accumulation and Ca^{2+}-dependent mito$O_2^{-\cdot}$ formation, as well as to the ensuing apoptosis driven by mitochondrial dysfunction. Although future studies should more carefully address this issue, we nevertheless note that experimental animal or human exposure to arsenite has been associated to mitochondrial ROS formation and toxicity in tissues as the heart (Flora 2011; Jomova et al. 2011; Abdul et al. 2015), brain (Flora 2011; Jomova et al. 2011; Abdul et al. 2015; Mochizuki 2019) and skeletal muscle (Ambrosio et al. 2014), in which RyR expression and function is well documented.

Materials and methods

Chemicals

Sodium arsenite, 2-aminoethoxydiphenyl borate (2-APB), Ry, caffeine (Cf), 4-chloro-m-cresol, ATP, 3-(4,5-dimethylthiazol-2-yl)-2,5-diphenyltetrazolium bromide (MTT), as well most of reagent-grade chemicals were purchased from Sigma-Aldrich (Milan, Italy). Ru360 was from Thermo Fisher Scientific (Milan, Italy). Fluo-4- acetoxymethyl ester (AM), Rhod 2-acetoxymethyl ester (AM), MitoSOX red, Dihydrorhodamine 123 (DHR) and MitoTracker Red CMXRos were purchased from Thermo Fisher Scientific. MitoTracker Deep Red tracker was purchased from Molecular probes (Leiden, The Netherlands).

Cell culture and treatment conditions

U937 human myeloid leukemia cells, herein defined as U-U937 cells, were cultured in suspension in RPMI 1640 medium (Sigma-Aldrich). Culture media were supplemented with 10% fetal bovine serum (FBS, Euroclone, Celbio Biotecnologie, Milan, Italy). These cells (U-U937) were differentiated to monocytes (D-U937) by a 4-day growth in culture medium supplemented with 1.3% DMSO as previous described (Guidarelli et al. 2009).

The mouse myoblast cell line C2C12 (ECACC 91031101, lot 12F005) was purchased from the European Collection of Authenticated Cell Cultures (ECACC, Salisbury, UK) and cultured in high-glucose D-MEM (Sigma-Aldrich) supplemented with 10% heat inactivated FBS, 2 mM L-glutamine (Euroclone). Cells at 60-70 % confluence were split 1:4 or 1:5. Upon 80-90% confluence, C2C12 myoblasts (U-C2C12) were stimulated to differentiate (D-C2C12) by changing the growth medium with D-MEM containing 1% heat inactivated FBS. Fresh D-MEM (1% heat inactivated FBS) was replaced daily. In all experiments reported in the present paper, C2C12 cells were used up to passage number 15.

HeLa human cervical cancer cells, were grown in Dulbecco's modified Eagle medium supplemented with 10% FBS (Euroclone). All cells were cultured with penicillin (100 units/ml), and streptomycin (100 mg/ml) (Euroclone) at 37° C in T-75 tissue culture flasks (Corning Inc., Corning, NY) gassed with an atmosphere of 95% air-5% CO_2.

Sodium arsenite was prepared as a 1 mM stock solution in saline A (8.182 g/l NaCl, 0.372 g/l KCl, 0.336 g/l $NaHCO_3$, and 0.9 g/l glucose, pH 7.4) and stored at 4° C. Cells (1.5 x 10^5 cells/ml) were exposed to arsenite, and/or other addictions, in the respective complete culture medium, as detailed in the text, as well as in the legends to the figures.

Measurement of intracellular free calcium levels and mitochondrial Ca^{2+}

HeLa, U-U937, D-U937, U-C2C12 or D-C2C12 cells were grown in 35 mm tissue culture dishes containing an uncoated coverslip, treated for 20 min with 4 μM Fluo 4-AM or 10 μM Rhod 2-AM and subsequently exposed for further 10 min to the indicated IP_3R or RyR agonists. In some experiments, the cells were exposed to arsenite for 6 h and Fluo 4-AM or Rhod 2-AM was added to the culture medium in the last 30 min. After the treatment the U-U937 or D-U937 cells were centrifuged and incubated for 10 min in 2 ml of saline A, that leads the cells to attach to the coverslip.

The cells were finally washed three times in PBS and fluorescence images were captured with a BX-51 microscope (Olympus, Milan, Italy), equipped with a SPOT-RT camera unit (Diagnostic Instruments, Delta Sistemi, Rome, Italy) using an Olympus LCAch 40 x/0.55 objective lens.

The excitation and emission wavelengths were 488 and 515 nm (Fluo 4), and 540 and 590 nm (Rhod 2) with a 5-nm slit width for both emission and excitation. Images were collected with exposure times of 100-400 ms, digitally acquired and processed for fluorescence determination at the single cell level by ImageJ software. Mean fluorescence values were determined by averaging the fluorescence values of at least 50 cells/treatment condition/experiment.

Super resolution and confocal microscopy

U-U937 and D-C2C12 cells were grown in arsenite for 6 h and Rhod 2-AM together with MitoTracker Deep Red tracker were added to the culture medium in the last 30 min. Confocal and Structured illumination microscopy (SIM) was done on a Nikon SIM system with a 100x 1.49 NA oil immersion objective, managed by NIS elements software. Raw and reconstructed images were validated with the SIM check plugin of Image. Four different fields were randomly selected throughout the wells and imaged at laser excitation of 561 nm (Rhod-2AM) and 640 nm (mitochondria with MitoTracker Deep Red) with a 3D-SIM acquisition protocol. Confocal images were quantified with ImageJ. Co-localisation between Rhod-2AM and MitoTracker was analyzed using the Jacop ImageJ plugin and expressed as Manders index.

DHR and MitoSOX red fluorescence assay

HeLa, U-U937, D-U937, U-C2C12 or D-C2C12 cells were grown in 35 mm tissue culture dishes containing an uncoated coverslip exposed for 30 min with either 5 μM MitoSOX red or 10 μM DHR prior to the end of the treatment with arsenite (6 h). After the treatment, U-U937 and D-U937 cells were centrifuged, incubated for 10 min in 2 ml of saline A and subsequently processed as described in (Guidarelli et al. 2019b).

Measurement of mitochondrial membrane potential

HeLa, U-U937, D-U937, U-C2C12 or D-C2C12 cells were grown in 35 mm tissue culture dishes containing an uncoated coverslip, exposed for 30 min with 50 nM MitoTracker Red CMXRos prior to the end of the treatment with arsenite (16 h). After the treatment, the U-U937 or D-U937 cells were centrifuged and incubated for 10 min in 2 ml of saline A.

The cells were finally washed three times and the fluorescence images were visualized using a fluorescence microscope. The excitation and emission wavelengths were 545 and 610 nm,

respectively, with a 5-nm slit width for both emission and excitation. Mean fluorescence values were determined by averaging the fluorescence values of at least 50 cells/treatment condition/experiment.

Immunofluorescence analysis

HeLa, U-U937, D-U937, U-C2C12 or D-C2C12 cells were grown in 35 mm tissue culture dishes containing an uncoated coverslip, incubated for 16 h in the absence or presence of arsenite. After the treatment, the U-U937 or D-U937 cells were centrifuged, incubated for 10 min in 2 ml of saline A and subsequently processed as described in (Guidarelli et al. 2019b).

Fluorogenic caspase 3 assay

HeLa, U-U937, D-U937, U-C2C12 or D-C2C12 cells were grown in 60 mm tissue culture, exposed for 24 h in the absence or presence of arsenite. After the treatments, the Caspase 3-like activity was monitored as described in (Guidarelli et al. 2019b). Briefly, the cells were lysed and aliquots of the extract (30 μg proteins) were incubated with 12 μM Ac-DEVD-AMC, at 30° C. Caspase 3-like activity was determined fluorometrically (excitation at 360 nm and emission at 460 nm) by quantifying the release of aminomethylcoumarin (AMC) from cleaved caspase 3 substrate (Ac-DEVD-AMC).

Cytotoxicity assay

HeLa, U-U937, D-U937, U-C2C12 or D-C2C12 cells were grown in 35 mm tissue culture, exposed for 24 h in the absence or presence of arsenite. After the treatment, the number of viable cells was estimated with the trypan blue exclusion assay. Briefly, an aliquot of the cell suspension was diluted 1:2 (v/v) with 0.4% trypan blue, and the viable cells (i.e., those excluding trypan blue) were counted using the hemocytometer.

In other experiments, the cells were supplemented with 25 μg/ml MTT at 37°C in 5% CO_2 30 min prior to the end of the treatment with arsenite (24 h). The medium was then removed and replaced

with 1 ml of dimethyl sulfoxide, and cell viability was assessed by measuring MTT reductase activity. Absorbance was read at 570 nm. Results are expressed as the percentage of MTT-reducing activity (absorbance in treated versus untreated cells).

Analysis of apoptosis with the Hoechst 33342 assay

HeLa, U-U937, D-U937, U-C2C12 or D-C2C12 cells were grown in 35 mm tissue culture, exposed for 24 h in the absence or presence of arsenite and subsequently incubated for 5 min with 10 μM Hoechst 33342. The cells were finally analysed with a fluorescence microscope to assess their nuclear morphology (chromatin condensation and fragmentation). Cells with homogeneously stained nuclei were considered viable.

Statistical analysis

The results are expressed as means ± S.D. Statistical differences were analysed by one-way analysis of variance (ANOVA) followed by Dunnett's test for multiple comparison or two-way ANOVA followed by Bonferroni's test for multiple comparison. We used unpaired *t* test for two group analysis. $P < 0.05$ was considered significant.

Declarations

Data availability

All data generated or analyzed during this study are included in this article.

Funding

This work was supported by Ministero dell'Università e della Ricerca Scientifica e Tecnologica, Programmi di Ricerca Scientifica di Rilevante Interesse Nazionale, 2017, [Grant number: 2017FJSM9S].

Conflict of interest

The authors declare no competing interests.

Ethics approval

Not applicable.

Consent to participate

Not applicable.

Consent for publication

Not applicable.

Code availability

Not applicable.

Contributions

AG and OC conceived the research. AG, MF, AS, AC, EV, SF and EZ performed the experiments. AG, MF, AS, AC and EZ analyzed the data. OC wrote the manuscript. AG, MF, AS, AC, EZ and OC analyzed manuscript. All authors approved the final version of the manuscript.

References

Abdul KS, Jayasinghe SS, Chandana EP, Jayasumana C, De Silva PM. Arsenic and human health effects: A review. Environ Toxicol Pharmacol 2015;40:828-846.

Airey JA, Baring MD, Sutko JL. Ryanodine receptor protein is expressed during differentiation in the muscle cell lines BC3H1 and C2C12. Dev Biol 1991;148:365-374.

Ambrosio F, Brown E, Stolz D, Ferrari R, Goodpaster B, Deasy B, Distefano G, Roperti A, Cheikhi A, Garciafigueroa Y, Barchowsky A. Arsenic induces sustained impairment of skeletal muscle and muscle progenitor cell ultrastructure and bioenergetics. Free Radic Biol Med 2014;74:64-73.

Angelova PR, Abramov AY. Functional role of mitochondrial reactive oxygen species in physiology. Free Radic Biol Med 2016;100:81-85.

Bansaghi S, Golenar T, Madesh M, Csordas G, Ramachandrarao S, Sharma K, Yule DI, Joseph SK, Hajnoczky G. Isoform- and species-specific control of inositol 1,4,5-trisphosphate (IP3) receptors by reactive oxygen species. J Biol Chem 2014;289:8170-8181.

Bennett DL, Cheek TR, Berridge MJ, De Smedt H, Parys JB, Missiaen L, Bootman MD. Expression and function of ryanodine receptors in nonexcitable cells. J Biol Chem 1996;271:6356-6362.

Berridge MJ. Inositol trisphosphate and calcium signalling. Nature 1993;361:315-325.

Berridge MJ. The Inositol Trisphosphate/Calcium Signaling Pathway in Health and Disease. Physiol Rev 2016;96:1261-1296.

Bhosale G, Sharpe JA, Sundier SY, Duchen MR. Calcium signaling as a mediator of cell energy demand and a trigger to cell death. Ann N Y Acad Sci 2015;1350:107-116.

Chang YY, Kuo TC, Hsu CH, Hou DR, Kao YH, Huang RN. Characterization of the role of protein-cysteine residues in the binding with sodium arsenite. Arch Toxicol 2012;86:911-922.

Clementi E, Guidarelli A, Cantoni O. The inositol 1,4,5-trisphosphate-generating agonist ATP enhances DNA cleavage induced by tert-butylhydroperoxide. Exp Cell Res 1998;239:175-178.

Denton RM. Regulation of mitochondrial dehydrogenases by calcium ions. Biochim Biophys Acta 2009;1787:1309-1316.

Flora SJ. Arsenic-induced oxidative stress and its reversibility. Free Radic Biol Med. 2011;51:257-281.

Gomes A, Fernandes E, Lima JL. Fluorescence probes used for detection of reactive oxygen species. J Biochem Biophys Methods 2005;65:45-80.

Guidarelli A, Cerioni L, Fiorani M, Cantoni O. Differentiation-associated loss of ryanodine receptors: a strategy adopted by monocytes/macrophages to prevent the DNA single-strand breakage induced by peroxynitrite. J Immunol 2009;183:4449-4457.

Guidarelli A, Fiorani M & Cantoni O (2018) Low Concentrations of Arsenite Target the Intraluminal Inositol 1, 4, 5-Trisphosphate Receptor/Ryanodine Receptor Crosstalk to Significantly Elevate Intracellular Ca^{2+}. J Pharmacol Exp Ther 2018;367:184-193.

Guidarelli A, Fiorani M, Cerioni L, Cantoni O. The compartmentalised nature of the mechanisms governing superoxide formation and scavenging in cells exposed to arsenite. Toxicol Appl Pharmacol 2019a;384:114766.

Guidarelli A, Fiorani M, Cerioni L, Cantoni O. Calcium signals between the ryanodine receptor- and mitochondria critically regulate the effects of arsenite on mitochondrial superoxide formation and on the ensuing survival vs apoptotic signaling. Redox Biol 2019b;20:285-295.

Guidarelli A, Cerioni L, Fiorani M, Catalani A, Cantoni O. Arsenite-Induced Mitochondrial Superoxide Formation: Time and Concentration Requirements for the Effects of the Metalloid on the Endoplasmic Reticulum and Mitochondria. J Pharmacol Exp Ther 2020;373:62-71.

Hosoi E, Nishizaki C, Gallagher KL, Wyre HW, Matsuo Y, Sei Y. Expression of the ryanodine receptor isoforms in immune cells. J Immunol 2001;167:4887-4894.

Hu Y, Li J, Lou B, Wu R, Wang G, Lu C, Wang H, Pi J, Xu Y. The Role of Reactive Oxygen Species in Arsenic Toxicity. Biomolecules 2020;10:240.

Jomova K, Jenisova Z, Feszterova M, Baros S, Liska J, Hudecova D, Rhodes CJ, Valko M. Arsenic: toxicity, oxidative stress and human disease. J Appl Toxicol 2011;31:95-107.

Kirichok Y, Krapivinsky G, Clapham DE. The mitochondrial calcium uniporter is a highly selective ion channel. Nature 2004;427:360-364.

Liu SX, Davidson MM, Tang X, Walker WF, Athar M, Ivanov V, Hei TK. Mitochondrial damage mediates genotoxicity of arsenic in mammalian cells. Cancer Res 2005;65:3236-3242.

Meissner G. The structural basis of ryanodine receptor ion channel function. J Gen Physiol 2017;149:1065-1089.

Minatel BC, Sage AP, Anderson C, Hubaux R, Marshall EA, Lam WL, Martinez VD. Environmental arsenic exposure: From genetic susceptibility to pathogenesis. Environ Int 2018;112:183-197.

Mochizuki H. Arsenic Neurotoxicity in Humans. Int J Mol Sci 2019;20:3418.

Mukhopadhyay P, Rajesh M, Hasko G, Hawkins BJ, Madesh M, Pacher P. Simultaneous detection of apoptosis and mitochondrial superoxide production in live cells by flow cytometry and confocal microscopy. Nat Protoc 2007;2:2295-2301.

Rizzuto R, De Stefani D, Raffaello A, Mammucari C. Mitochondria as sensors and regulators of calcium signalling. Nat Rev Mol Cell Biol 2012;13:566-578.

Shen S, Li XF, Cullen WR, Weinfeld M, Le XC. Arsenic binding to proteins. Chem Rev 2013;113:7769-7792.

Smith KR, Klei LR, Barchowsky A. Arsenite stimulates plasma membrane NADPH oxidase in vascular endothelial cells. Am J Physiol Lung Cell Mol Physiol 2001;280:L442-449.

Straub AC, Clark KA, Ross MA, Chandra AG, Li S, Gao X, Pagano PJ, Stolz DB, Barchowsky A. Arsenic-stimulated liver sinusoidal capillarization in mice requires NADPH oxidase-generated superoxide. J Clin Invest 2008;118:3980-3989.

Sugiyama T, Yamamoto-Hino M, Miyawaki A, Furuichi T, Mikoshiba K, Hasegawa M. Subtypes of inositol 1,4,5-trisphosphate receptor in human hematopoietic cell lines: dynamic aspects of their cell-type specific expression. FEBS Lett 1994;349:191-196.

Tarroni P, Rossi D, Conti A, Sorrentino V. Expression of the ryanodine receptor type 3 calcium release channel during development and differentiation of mammalian skeletal muscle cells. J Biol Chem 1997;272:19808-19813.

Van Petegem F (2012) Ryanodine receptors: structure and function. J Biol Chem 2012;287:31624-31632.

Weisiger RA, Fridovich I. Mitochondrial superoxide simutase. Site of synthesis and intramitochondrial localization. J Biol Chem 1973;248:4793-4796.

Zazueta C, Sosa-Torres ME, Correa F, Garza-Ortiz A. Inhibitory properties of ruthenium amine complexes on mitochondrial calcium uptake. J Bioenerg Biomembr 1999;31:551-557.

Legend to the figures

Fig. 1. Characterization of the Ca^{2+} responses mediated by IP_3R and RyR agonists in HeLa, U-U937, D-U937, U-C2C2 and D-C2C12 cells. HeLa, U-U937, D-U937, U-C2C12 and D-C2C12 cells were pre-exposed for 20 min to Fluo 4-AM and then treater for 10 min with 10 mM Cf (**a**) or 100 μM ATP (**b**). In some experiments, 50 μM 2-APB, or 20 μM Ry, was added to the cultures 5 min prior to Cf or ATP. After treatments, the cells were analysed for Fluo 4-fluorescence. The results represent the means ± SD calculated from at least three distinct experiments. *P <0.05, **P <0.01, as compared to untreated cells. (*)P < 0.05, (**)P < 0.01, as compared to cells treated with agonists (ANOVA followed by Dunnett's test).

Fig. 2. Arsenite induces different Ca^{2+} responses in cells expressing the IP_3R, with or without concomitant RyR expression. (**a**) HeLa, U-U937, D-U937, U-C2C12 and D-C2C12 cells were pre-exposed for 5 min to the vehicle, 2-APB or Ry and subsequently incubated for 6 h in the presence of 2.5 μM arsenite. After treatments, the cells were analysed for Fluo 4-fluorescence. The results represent the means ± SD calculated from at least three distinct experiments. *P <0.05, **P <0.01, as compared to untreated cells. (*)P < 0.05, (**)P < 0.01, as compared to cells treated with arsenite (ANOVA followed by Dunnett's test). (**b**) Each of the above cell lines was exposed for 6 h to increasing concentrations of arsenite and finally analysed for Fluo 4-fluorescence. The effect of Ry was tested in U-U937 and D-C2C12 cells. The results represent the means ± SD calculated from at least three distinct experiments. *P <0.05, **P <0.01, ***P <0.001, as compared to untreated cells (two-way ANOVA followed by Bonferroni's test).

Fig. 3. ATP stimulation increases the mitochondrial accumulation of Ca^{2+} in cells expressing the IP_3R, with or without concomitant RyR expression. HeLa (**a**), U-U937 (**b**), D-U937 (**c**), U-C2C12 (**d**) and D-C2C12 (**e**) cells were pre-exposed for 5 min to the vehicle, 10 μM Ru-360, 2-APB or Ry and treated for a further 10 min with 100 μM ATP. After treatments, the cells were analysed for Rhod 2-fluorescence. The results represent the means ± SD calculated from at least three distinct

experiments. * P <0.01, as compared to untreated cells. (*)P < 0.01, as compared to cells treated with ATP (ANOVA followed by Dunnett's test).

Fig. 4. Arsenite fails to increase the mitochondrial concentration of Ca^{2+} in cells uniquely expressing the IP_3R. HeLa (**a**), U-U937 (**b**), D-U937 (**c**), U-C2C12 (**d**) and D-C2C12 (**e**) cells were pre-exposed for 5 min to the vehicle, Ru-360, 2-APB or Ry and incubated for a further 6 h in the presence of 2.5 μM arsenite. After treatments, the cells were analysed for Rhod 2-fluorescence. The results represent the means ± SD calculated from at least three distinct experiments. * P <0.01, as compared to untreated cells. (*)P < 0.01, as compared to cells treated with arsenite (ANOVA followed by Dunnett's test). (**f**) Cells were incubated with increasing concentrations of arsenite for 6 h. After treatments, the cells were analysed for Rhod 2-fluorescence. The results represent the means ± SD calculated from at least three distinct experiments. (N.d., not detectable). *P <0.01, **P <0.001, as compared to untreated cells (two-way ANOVA followed by Bonferroni's test). (**g**) D-C2C12 cells were incubated for 6 h with or without 2.5μM arsenite. After treatments, the cells were analysed to determine the co-localization of Rhod 2-AM (green) and MitoTracker Deep Red (red) fluorescence signals. On the right, panels display the merged image of the two stains. (**h**) Manders coefficient of Rhod 2-fluorescence in mitochondria was calculated as the proportion of Rhod 2-fluorescence signal overlapping with the signal of the Mitotracker in four randomly acquired fields. The results represent the means ± SD.*P <0.05 as compared to untreated cells (Two-tailed unpaired t test). (**i**) High Resolution SIM images of Mitotracker signal (green) and Rhod 2-AM (red) in D-C2C12 cells. Insets represent area where Rhod 2-AM signal colocalises with that of the Mitotracker in arsenite-treated D-C2C12.

Fig. 5. Arsenite fails to induce $mitoO_2^{\cdot-}$ formation in cells with only IP_3R. HeLa (**a**, **b**), U-U937 (**c**, **d**), D-U937 (**e**, **f**), U-C2C12 (**g**, **h**) and D-C2C12 (**i**, **j**) cells were pretreated for 5 min with the vehicle, Ru-360, 2-APB or Ry and incubated for 6 h with the further addition of 2.5 μM arsenite. After treatments, the cells were analysed for DHR- (**a-i**) or MitoSOX red (**b**-**j**)-fluorescence. The results

represent the means ± SD calculated from at least three distinct experiments. (N.d., not detectable). *P <0.01, as compared to untreated cells. (*)P < 0.01, as compared to cells treated with arsenite (ANOVA followed by Dunnett's test).

Fig. 6. ATP promotes mito$O_2^{-\cdot}$ formation in response to arsenite in cells uniquely expressing the IP_3R. HeLa, D-U937 and U-C2C12 cells were incubated for 6 h with 2.5 μM arsenite, rinsed and re-suspended in fresh culture medium containing the vehicle, Ru360, 2-APB or Ry. After 5 min, cells received 100 μM ATP for a further 10 min and were finally analyzed for MitoSOX red fluorescence. The results represent the means ± SD calculated from at least three distinct experiments. * P <0.01, as compared to untreated cells (ANOVA followed by Dunnett's test).

Fig. 7. Arsenite causes mitochondrial dysfunction and apoptosis in cells with both IP_3R and RyR. HeLa (**a**), U-U937 (**b**), D-U937 (**c**), U-C2C12 (**d**) and D-C2C12 (**e**) cells were treated for 16 (**a**-**e**i-ii) or 24 (**a**-**e**iii-vi) h with arsenite. After treatments, the cells were analysed for MitoTracker red CMXRos-fluorescence (**a**-**e**i), cytochrome c localization (**a**-**e**ii), caspase 3 activity (**a**-**e**iii), MTT reducing activity (**a**-**e**iv) and toxicity by either quantifying the number of viable cells (**a**-**e**v) or measuring chromatin fragmentation/condensation (**a**-**e**vi). The results represent the means ± SD calculated from at least three distinct experiments. * P <0.01, as compared to untreated cells (ANOVA followed by Dunnett's test).

Figures

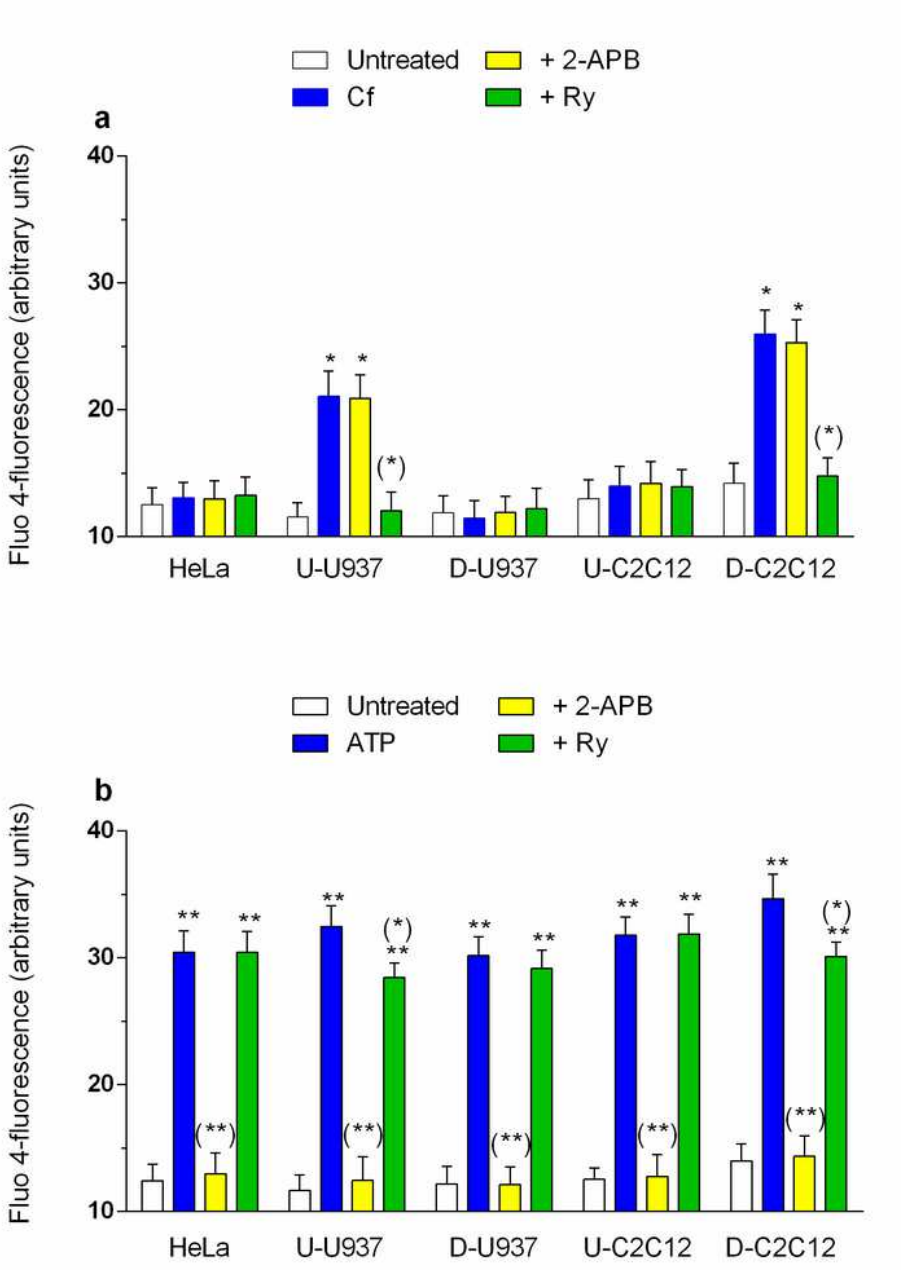

Fig. 1

Figure 1

Characterization of the Ca2+ responses mediated by IP3R and RyR agonists in HeLa, U-U937, D-U937, U-C2C2 and D-C2C12 cells. HeLa, U-U937, D-U937, U-C2C12 and D-C2C12 cells were pre-exposed for 20 min to Fluo 4-AM and then treater for 10 min with 10 mM Cf (a) or 100 μM ATP (b). In some experiments, 50

μM 2-APB, or 20 μM Ry, was added to the cultures 5 min prior to Cf or ATP. After treatments, the cells were analysed for Fluo 4-fluorescence. The results represent the means ± SD calculated from at least three distinct experiments. *P <0.05, **P <0.01, as compared to untreated cells. (*)P < 0.05, (**)P < 0.01, as compared to cells treated with agonists (ANOVA followed by Dunnett's test).

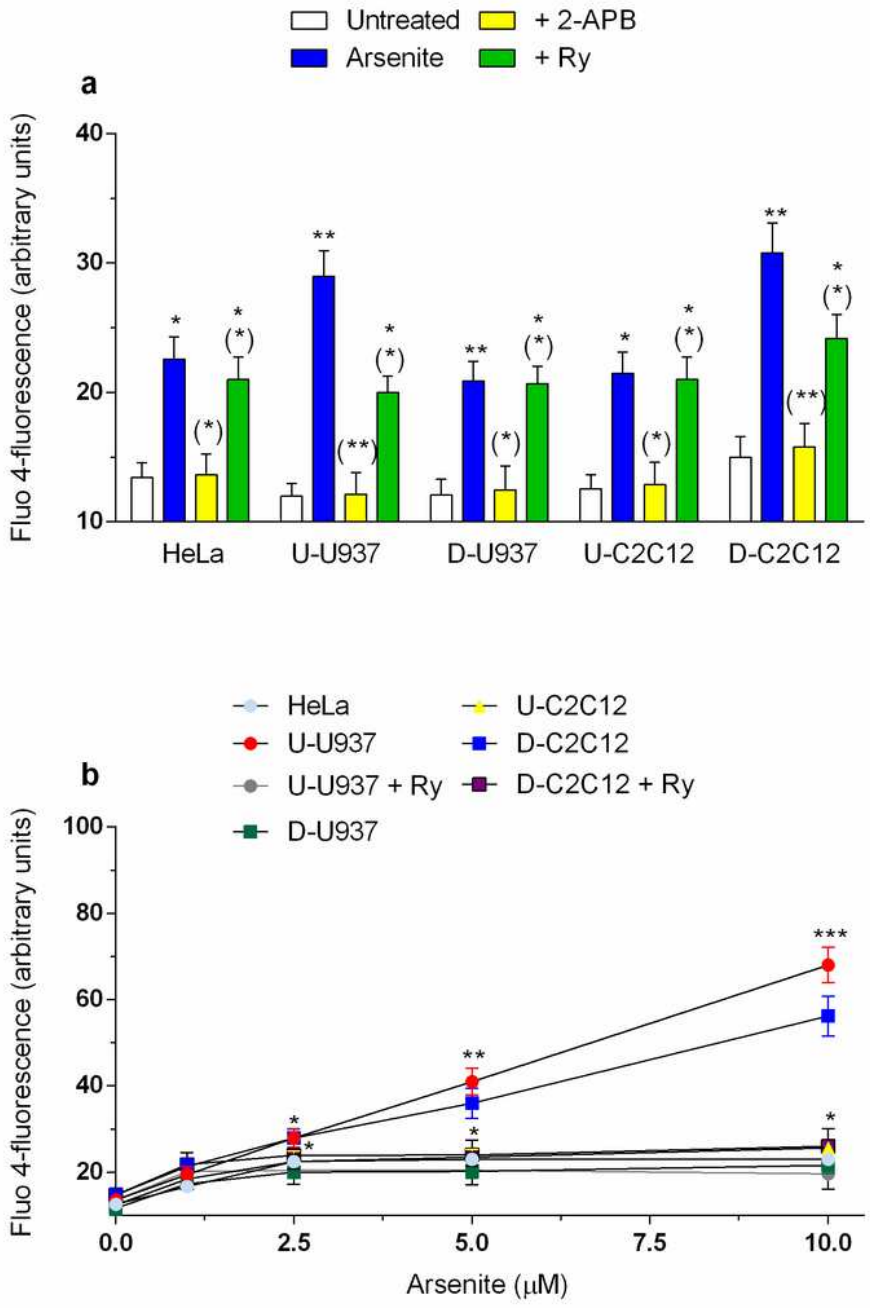

Fig. 2

Figure 2

Arsenite induces different Ca2+ responses in cells expressing the IP3R, with or without concomitant RyR expression. (a) HeLa, U-U937, D-U937, U-C2C12 and D-C2C12 cells were preexposed for 5 min to the vehicle, 2-APB or Ry and subsequently incubated for 6 h in the presence of 2.5 μM arsenite. After treatments, the cells were analysed for Fluo 4-fluorescence. The results represent the means ± SD calculated from at least three distinct experiments. *P <0.05, **P <0.01, as compared to untreated cells. (*)P < 0.05, (**)P < 0.01, as compared to cells treated with arsenite (ANOVA followed by Dunnett's test). (b) Each of the above cell lines was exposed for 6 h to increasing concentrations of arsenite and finally analysed for Fluo 4-fluorescence. The effect of Ry was tested in U-U937 and D-C2C12 cells. The results represent the means ± SD calculated from at least three distinct experiments. *P <0.05, **P <0.01, ***P <0.001, as compared to untreated cells (two-way ANOVA followed by Bonferroni’s test)

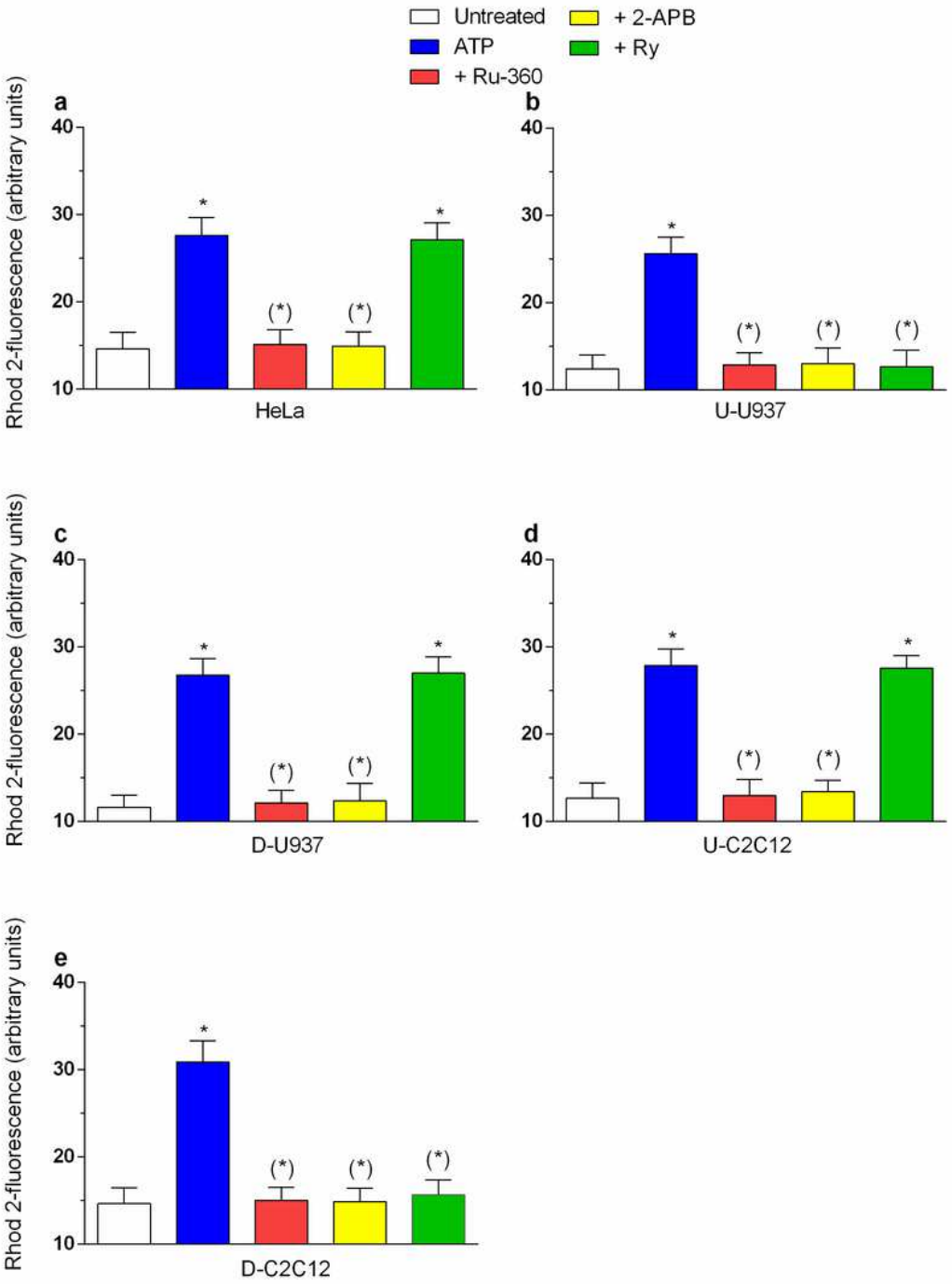

Fig. 3

Figure 3

ATP stimulation increases the mitochondrial accumulation of Ca2+ in cells expressing the IP3R, with or without concomitant RyR expression. HeLa (a), U-U937 (b), D-U937 (c), U-C2C12 (d) and D-C2C12 (e) cells were pre-exposed for 5 min to the vehicle, 10 μM Ru-360, 2-APB or Ry and treated for a further 10 min with 100 μM ATP. After treatments, the cells were analysed for Rhod 2-fluorescence. The results represent the

means ± SD calculated from at least three distinct 37 experiments. * P <0.01, as compared to untreated cells. (*)P < 0.01, as compared to cells treated with ATP (ANOVA followed by Dunnett's test).

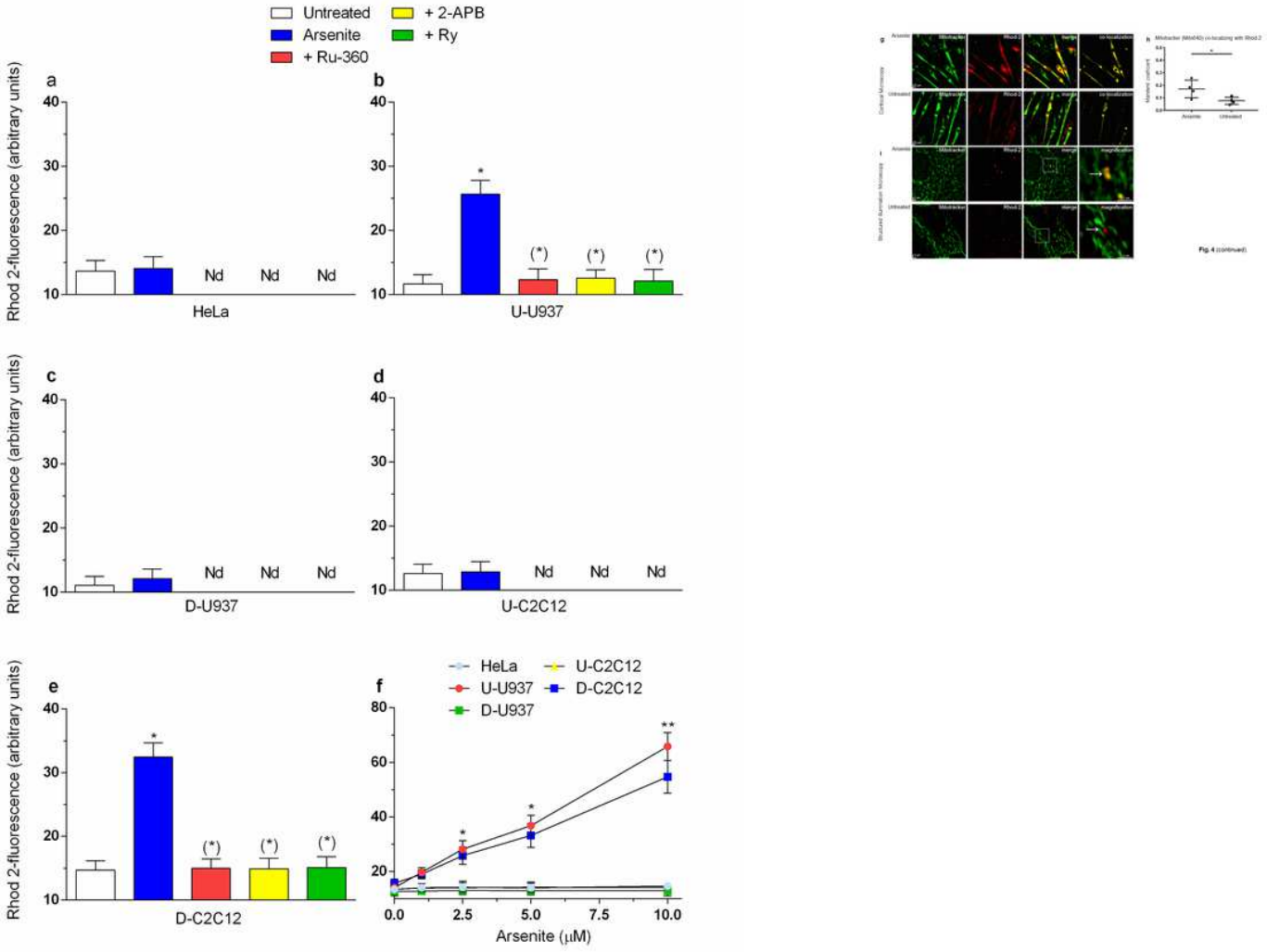

Fig. 4

Figure 4

Arsenite fails to increase the mitochondrial concentration of Ca2+ in cells uniquely expressing the IP3R. HeLa (a), U-U937 (b), D-U937 (c), U-C2C12 (d) and D-C2C12 (e) cells were pre-exposed for 5 min to the vehicle, Ru-360, 2-APB or Ry and incubated for a further 6 h in the presence of 2.5 μM arsenite. After treatments, the cells were analysed for Rhod 2-fluorescence. The results represent the means ± SD calculated from at least three distinct experiments. * P <0.01, as compared to untreated cells. (*)P < 0.01, as compared to cells treated with arsenite (ANOVA followed by Dunnett's test). (f) Cells were incubated with increasing concentrations of arsenite for 6 h. After treatments, the cells were analysed for Rhod 2-fluorescence. The results represent the means ± SD calculated from at least three distinct experiments. (N.d., not detectable). *P <0.01, **P <0.001, as compared to untreated cells (two-way ANOVA followed by Bonferroni's test). (g) D-C2C12 cells were incubated for 6 h with or without 2.5μM arsenite. After treatments, the cells were analysed to determine the co-localization of Rhod 2-AM (green) and

MitoTracker Deep Red (red) fluorescence signals. On the right, panels display the merged image of the two stains. (h) Manders coefficient of Rhod 2-fluorescence in mitochondria was calculated as the proportion of Rhod 2-fluorescence signal overlapping with the signal of the Mitotracker in four randomly acquired fields. The results represent the means ± SD.*P <0.05 as compared to untreated cells (Two-tailed unpaired t test). (i) High Resolution SIM images of Mitotracker signal (green) and Rhod 2-AM (red) in D-C2C12 cells. Insets represent area where Rhod 2-AM signal colocalises with that of the Mitotracker in arsenite-treated D-C2C12.

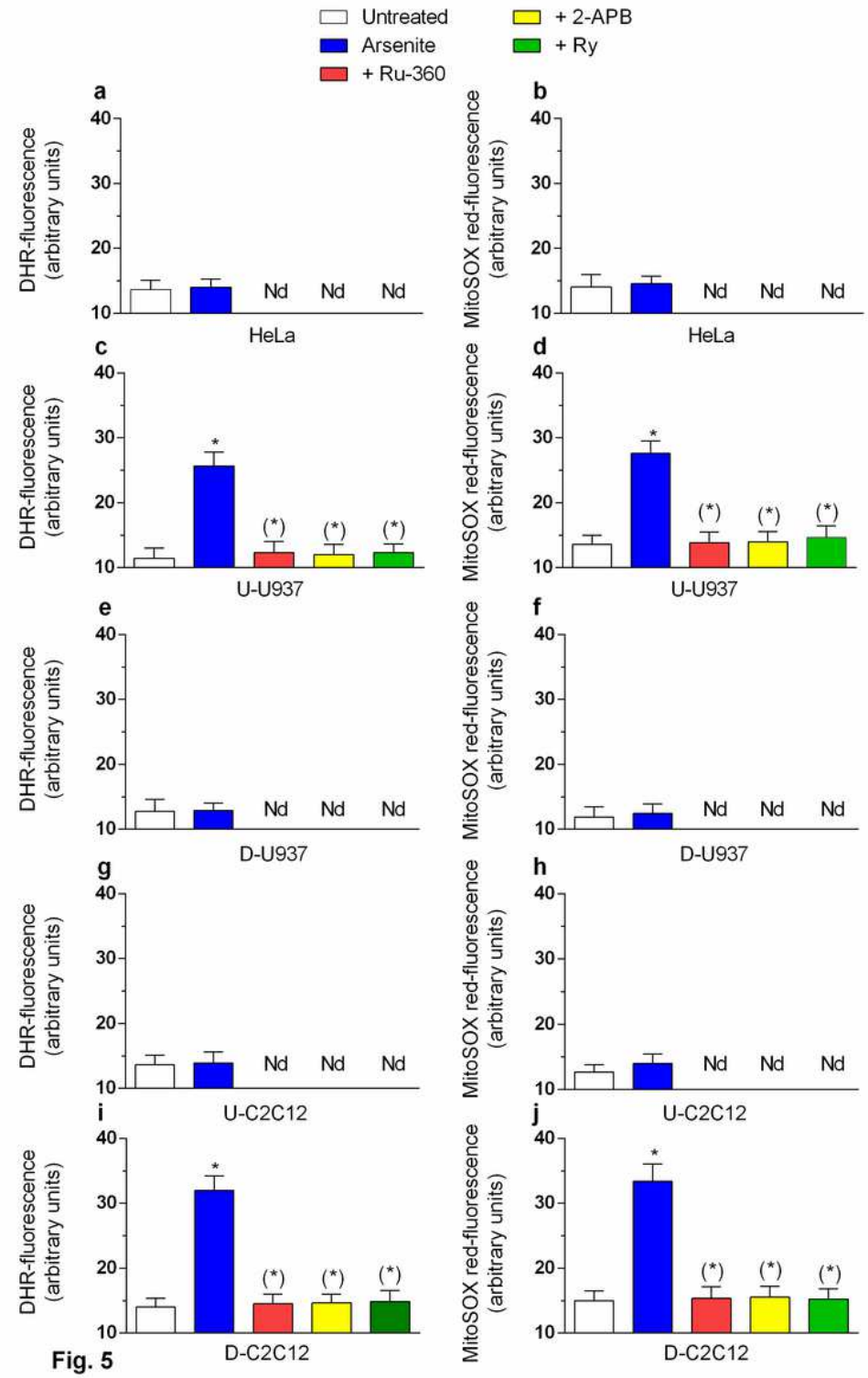

Fig. 5

Figure 5

Arsenite fails to induce mitoO2 -. formation in cells with only IP3R. HeLa (a, b), U-U937 (c, d), D-U937 (e, f), U-C2C12 (g, h) and D-C2C12 (i, j) cells were pretreated for 5 min with the vehicle, Ru-360, 2-APB or Ry and incubated for 6 h with the further addition of 2.5 μM arsenite. After treatments, the cells were analysed for DHR- (a-i) or MitoSOX red (b-j)-fluorescence. The results 38 represent the means ± SD calculated from at least three distinct experiments. (N.d., not detectable). *P <0.01, as compared to untreated cells. (*)P < 0.01, as compared to cells treated with arsenite (ANOVA followed by Dunnett's test).

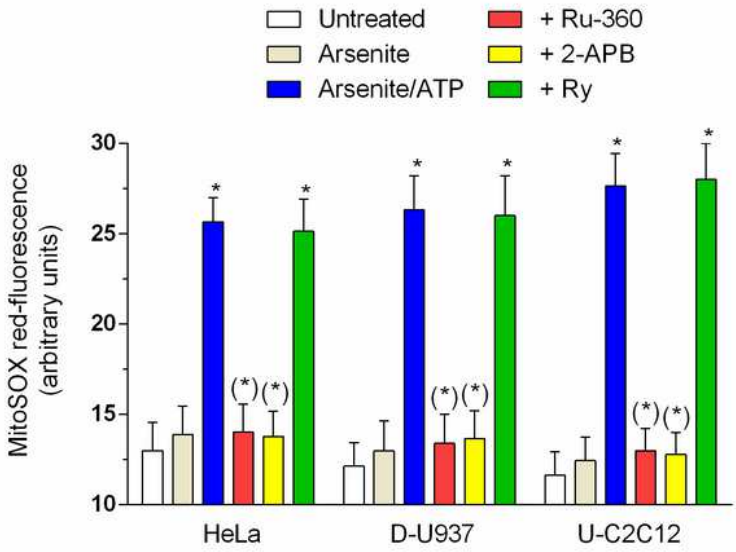

Fig. 6

Figure 6

ATP promotes mitoO2 -. formation in response to arsenite in cells uniquely expressing the IP3R. HeLa, D-U937 and U-C2C12 cells were incubated for 6 h with 2.5 µM arsenite, rinsed and resuspended in fresh culture medium containing the vehicle, Ru360, 2-APB or Ry. After 5 min, cells received 100 µM ATP for a further 10 min and were finally analyzed for MitoSOX red fluorescence. The results represent the means ± SD calculated from at least three distinct experiments. * P <0.01, as compared to untreated cells (ANOVA followed by Dunnett's test).

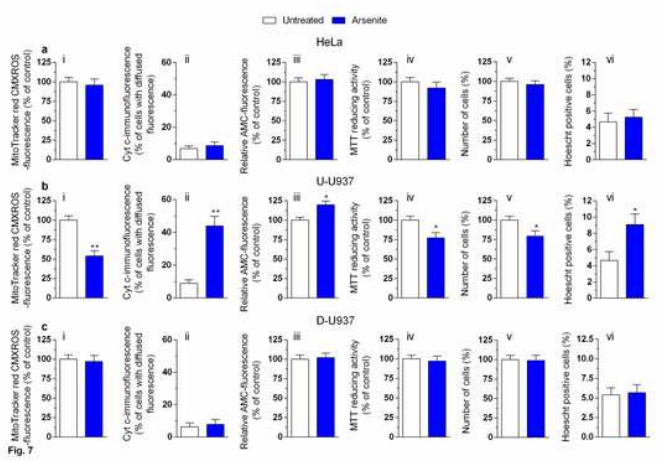

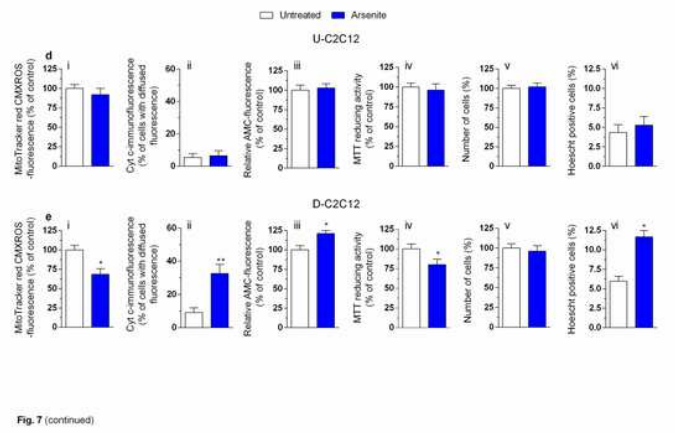

Figure 7

Arsenite causes mitochondrial dysfunction and apoptosis in cells with both IP3R and RyR. HeLa (a), U-U937 (b), D-U937 (c), U-C2C12 (d) and D-C2C12 (e) cells were treated for 16 (a-eiii) or 24 (a-eiii-vi) h with arsenite. After treatments, the cells were analysed for MitoTracker red CMXRos-fluorescence (a-ei), cytochrome c localization (a-eii), caspase 3 activity (a-eiii), MTT reducing activity (a-eiv) and toxicity by either quantifying the number of viable cells (a-ev) or measuring chromatin fragmentation/condensation (a-evi). The results represent the means ± SD calculated from at least three distinct experiments. * P <0.01, as compared to untreated cells (ANOVA followed by Dunnett's test)

Supplementary Files

This is a list of supplementary files associated with this preprint. Click to download.

- SupplementaryFig1.pdf